

Anthropogenic soils and sediments from historical trade hub on the bank of Morava River in Uherské Hradiště (Czech Republic): Archives of mediaeval landscape, environment and settlement dynamics[☆]

Katarína Adameková ^{a,b,*}, Jaroslav Bartík ^a, Jan Petřík ^b, Yannick Devos ^c, Libor Petr ^d, Petr Kočář ^{e,f}, Romana Kočárová ^d, Tomáš Chrátek ^g, Marcin Frączek ^h, Michal Kurka ⁱ, Miloslav Pouzar ^{i,j}

^a Institute of Archaeology of the Czech Academy of Sciences Čechyňská 363/19, Brno 602 00, Czech Republic

^b Department of Geological Science, Faculty of Sciences, Masaryk University, Kotlářská 2, Brno 61137, Czech Republic

^c Archaeology, Environmental Changes and Geo-Chemistry Research Group, Vrije Universiteit Brussel, Pleinlaan 2, Brussels 1050, Belgium

^d Department of Botany and Zoology, Faculty of Science, Masaryk University, Kotlářská 2, Brno 61137, Czech Republic

^e Institute of Archaeology of the Czech Academy of Sciences, Letenská 4, Praha 11801, Czech Republic

^f Department of Archaeology, Faculty of Arts, University of West Bohemia, Sedláčkova 15, Pilsen 30100, Czech Republic

^g The Museum of Moravian Slovakia, Smetanovy sady 179, Uherské Hradiště 68601, Czech Republic

^h Institute of Geography and Environmental Sciences, Department of Geomorphology and Geoarchaeology, Jan Kochanowski University in Kielce, Uniwersytecka 7 st, Kielce 25406, Poland

ⁱ Center of Materials and Nanotechnologies, Faculty of Chemical Technology, University of Pardubice, nam. Cs. legii 565, Pardubice 53002, Czech Republic

^j Environmental Chemistry and Toxicology Group, Institute of Environmental and Chemical Engineering, Faculty of Chemical Technology, University of Pardubice, Studentská 573, Pardubice 53210, Czech Republic

ARTICLE INFO

ABSTRACT

Keywords:
Pedogenesis
Dark Earth
Floodplain sediments
Marketplace
Early Mediaeval period
Soil micromorphology

This paper underscores the importance of investigating soils and sediments in proto-urban to urban archaeological contexts to gain a comprehensive understanding of their genesis and evolution, and their informative role in deciphering historical human–environment interactions and spatial organisation patterns. We focus on Early to High Mediaeval (6th–14th century CE) anthropogenically modified soils and sediments from Uherské Hradiště (Czech Republic). A study of well-preserved Dark Earths (DEs) uncovered in the Morava River floodplain allowed us to define interactions between people and their environment and to understand landscape evolution of the island area in relation to floodplain dynamics. A multi-proxy approach based on a combination of archaeological evidence, soil micromorphology, and physical, geochemical and palaeobotanical analyses, supplemented with dating methods was used to unravel the processes contributing to DE formation, human activities and the use of space. Initial settlement activities began in Uherské Hradiště at the end of the 7th or beginning of the 8th century CE, with later DEs indicating intensified human impact through craft activities, probably linked to market exchange from the 8th century, and even a possible marketplace underscoring its strategic importance within the broader economic and social networks, partially before and mainly during the Great Moravian period, in the 9th century CE. After a hiatus in the 10th–12th centuries AD, the site saw re-establishment in the 13th century CE, marking the early formation of the urbanisation in Uherské Hradiště. Despite repeated flooding, the settlement in the area was renewed repeatedly. Together with evidence of long-distance trade, this proves the importance of the place located on the commercial waterway of the Morava River. New findings reveal that this settlement could have played a more essential role in the Early Mediaeval era than previously expected.

[☆] This article is part of a special issue entitled: 'Soil Memory' published in Catena.

* Corresponding author at: Institute of Archaeology of the Czech Academy of Sciences, Čechyňská 363/19, 602 00 Brno, Czech Republic.

E-mail address: adamekova@arub.cz (K. Adameková).

1. Introduction

Dynamic fluvial networks and seasonal floods played crucial roles in shaping the landscape of the floodplain regions of mediaeval Europe. It was here that natural processes intersected with the long-term continuity of settlement and trade, significantly influencing the development of proto-urban and urban landscapes. This often led to repeated accumulation of cultural deposits, particularly in areas with concentrated commercial or craftwork activities (e.g. Devos et al., 2013a; Wouters et al., 2019). These areas therefore often exhibit a complex stratigraphy comprising alluvial and occupation deposits, the latter reflecting extensive human activities (e.g. Tys and Wouters, 2016; Khamnueva-Wendt et al., 2020). Such activities can lead to modifications and enrichment of soils and sediments (e.g. Cook and Heizer, 1965; Holliday, 2004) resulting in the formation of anthropogenically altered soils, known as Anthrosols or Technosols (IUSS Working Group WRB, 2022).

Such profoundly human-modified soils have already started forming in Europe several centuries ago in intensely inhabited proto-urban or urban environments. Particular attention has been paid to the so-called Dark Earths (DEs). They are characterised as relatively thick, dark, humic, no or weakly stratified and particularly homogenous horizons often containing anthropogenic materials such as fragments of pottery, bones, charcoals, plaster, bricks etc. that developed as a result of the interplay between human activity and natural syn- and post-depositional events (Nicosia et al., 2017). Therefore, their examination can reveal past environmental/palaeoecological changes, human activities and settlement patterns (e.g. Macphail et al., 1983; 2010; Nicosia et al., 2014; Nicosia et al., 2017; Borderie et al., 2015; Devos, 2019; Devos et al., 2022). The term Dark Earths has been used for the last decades as a descriptive rather than interpretative term as it has been demonstrated that every DE needs to be examined separately to fully understand its significant differences, considering the unique archaeological and societal circumstances (e.g. Macphail et al., 1994; Devos, 2019; Devos et al., 2022). Over the last decades DEs have been studied in urban archaeological contexts mainly in western, north-western, southwestern Europe and western Central Europe, where research has been ongoing for several decades and is constantly progressing (e.g. Macphail et al., 1994; Cammas et al., 2004; Borderie, 2011; Nicosia et al., 2012; Devos et al., 2013b; Wouters et al., 2017; Wouters et al., 2019; Bortolini et al., 2022; Grau-Sologestoa et al., 2023; Bortolini et al., 2024), while in eastern Central Europe research is limited to a few case studies (Krupski et al., 2017; Asare et al., 2020), none of them situated in alluvial settings.

The proto-urban development of Uherské Hradiště (Czech Republic, Central Europe) in Early Mediaeval Ages and the site's transformation into an urban space in the 13th century CE (Mitáček and Procházka, 2007) are still poorly understood because the remnants of the Great Moravian settlement and older occupation phases are deeply buried beneath urban constructions, accessible only in specific areas during new constructions, reconstructions, and linear trenches for engineering networks (e.g. Procházka and Snášil, 1983; Snášil and Procházka, 1984; Snášil and Novotný, 1985; Procházka, 1999; Menoušková, 2008). Furthermore, some of the findings were irretrievably lost in a 20th-century flood that affected the depository of Uherské Hradiště (Frolíková-Kaliszová, 2020). A recent archaeological excavation of the cellar of one of the modern buildings in the actual town centre revealing a sequence of floodplain sediments and DEs offers a unique opportunity to fill in some of the missing pieces.

We aim to: 1) understand how DEs at Uherské Hradiště were formed, focusing on the interplay between soil formation, floodplain environment evolution, and settlement activities, 2) reconstruct the ancient Mediaeval environment and changes over time based on palynological and archaeobotanical evidence, and 3) interpret archaeological findings from recent excavations and integrate it with the genesis of the DE to understand past human activities and settlement patterns from the proto-urban to urban development of Uherské Hradiště and discuss it in

a wider context.

2. Regional settings

2.1. Site description

Uherské Hradiště (49.0703886 N, 17.4599381 E, Czech Republic) is located approximately 80 km to the southeast of the city of Brno, Moravia region, in the floodplain of the Morava River, which is a part of the geomorphological formation of the Lower Morava Valley that belongs to the northernmost part of the Vienna Basin (Fig. 1A). The Morava River flows here between the Chřiby highlands in the west and the Vizovice Hills in the east. During the late Pleistocene, it formed a system of islands on the river sands, which were covered by overbank fluvial sediments in the Holocene (e.g. Procházka and Havlíček, 1996). The town Uherské Hradiště was built on the island of St. George (Fig. 2A) which was originally interwoven with channels that were modified by man since the Middle Ages (Procházka and Sulitková, 1984). The island is composed of various types of fluvial sediments and anthropogenic deposits. Quaternary sediments such as colluvium and loess deposits are also found in the surrounding area of the island (Fig. 1B). The floodplain is surrounded by low hills of the Carpathian Flysch Belt formed mainly by sandstone and claystone from the Magura Nappe-group. Except for the Anthrosols occurring on the studied site and in the wider area of the town itself, Fluvisols, Gleysols and Greyic Phaeozems developed in the floodplain. Recent soils in the surrounding upland include Chernozems, Luvisols and Cambisols (Fig. 1C). The current average annual air temperature is in the range of 8 °C–9 °C, and the total average annual precipitation is in the range of 450–550 mm (Tolasz, 2007). The studied sedimentary sequences were discovered during an archaeological rescue excavation in 2017 (Bartík and Chrátek, 2018; Petřík et al., 2018) in the northeastern corner of Mariánské Square in the cellar of house No. 125 (Fig. 2B, 2C). The altitude of the current surface reaches 181 m a.s.l. The youngest part of the preserved record was captured 270–280 cm deep below rubble and recent building foundations.

2.2. Archaeological and historical context of Uherské Hradiště

The island of St. George, on which the stone fortifications of the newly established city Uherské Hradiště were erected in the 13th century CE, lay on an ancient trade route (the Amber Road's eastern branch) connecting southern Europe to the Baltic Sea, and there was also an essential ford across the Morava River (Hrubý, 1957; Snášil, 1971). During the Early Mediaeval Ages, the island of St. George, together with the nearby Staré Město city (Fig. 2A), was a part of a large residential agglomeration (Galuška, 1999; Galuška and Kouril, 2014). It was one of several documented (sub)urban agglomerations with a central function (Galuška and Poláček, 2006). During the 9th century CE, the aforementioned agglomerations served as the administrative, cultural and economic centres of the pre-state entity known as 'Great Moravia' (Měřinský, 2006). The exact function of the island of St. George within the said agglomeration has not yet been resolved. However, the occurrence of prestigious artefacts that confirm the presence of the social elite and the abundant remains of the stone mortar buildings indicate the central function of the island. Although the remains of an Early Mediaeval settlement have been identified in almost two dozen locations (cf. Procházka and Havlíček, 1996; Frolíková-Kaliszová, 2020; Menoušková, 2020), we still have only fragmentary information on the settlement structure. We can get a certain idea of the character of the development based on housing estates investigated in the nearby Staré Město city (Hrubý, 1965) or in Uherské Hradiště-Sady (Marešová, 1985) (Fig. 2A). Typical residential buildings in the form of partially sunken dugouts or log cabins with heating equipment in the corner were documented on these settlements, which complemented other economic (storage pits, barns, haylofts and furnaces) and production facilities (forge, specialised workshop, etc.). The specifics of the island of St. George are findings

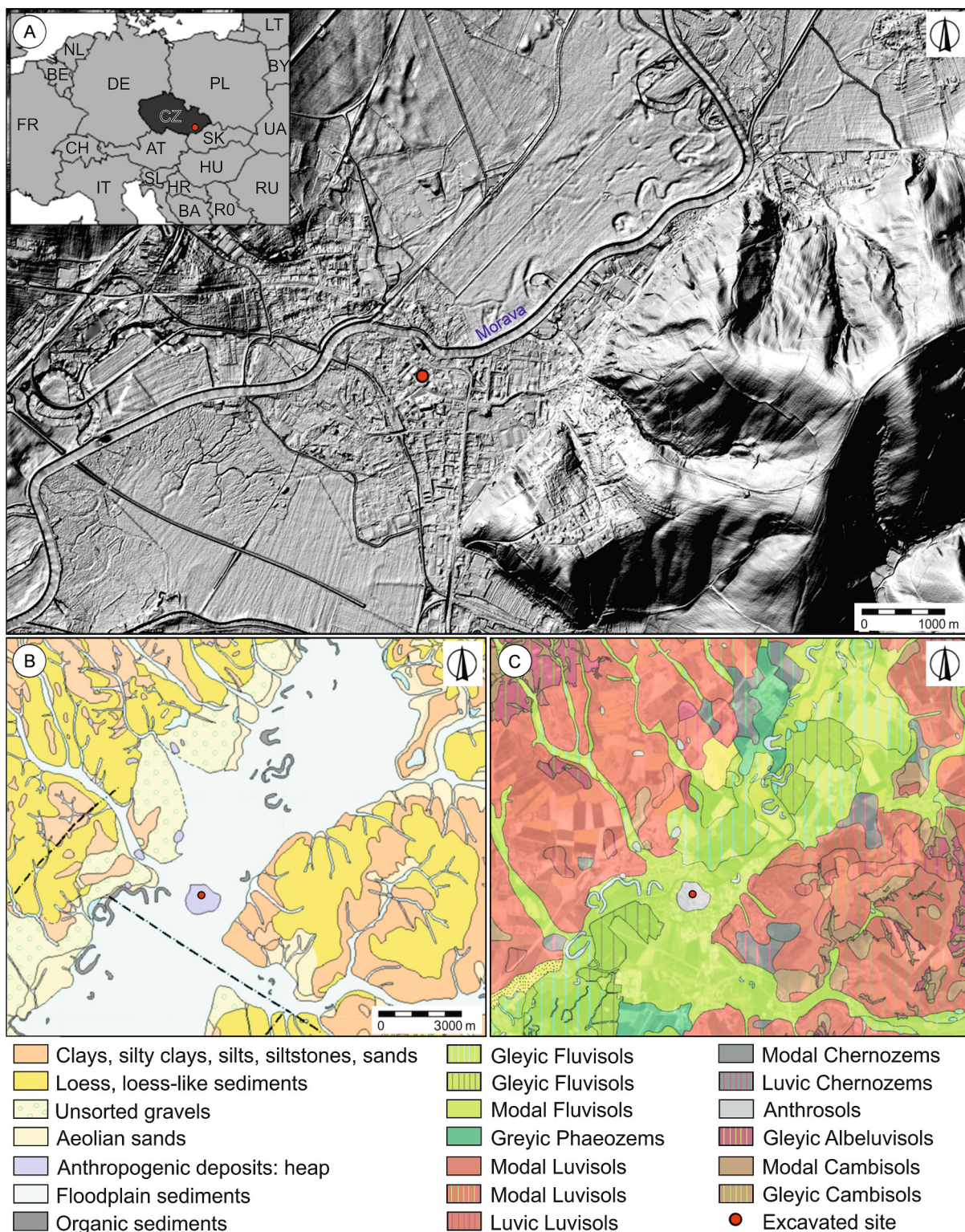


Fig. 1. A – Position of the studied site Uherské Hradiště (WGS 84: 49.0703886 N, 17.4599381E) within Europe and on the floodplain of the Morava River (in the Lower Morava Valley) shown on a digital elevation model (copyright by State Administration of Land Surveying and Cadastre). B – Geological map of the studied area (copyright by Czech Geological Survey). C – Pedological map of the area of interest (copyright by Czech Geological Survey).

from the destruction of buildings made of stone and mortar, most of which were probably of a profane nature (Snášil and Procházka, 1981; 1982; 1984; Snášil and Novotný, 1985; Menoušková 2020; Menoušková et al., 2019). However, the existence of two sacred buildings is also assumed (Kohoutek and Procházka, 1993; 1997; Dresler and Vágner, 2013).

3. Material and methods

3.1. Field observations

The investigated area (ca. 300 m²) was divided into several parts marked as Room 1 to Room 6 (Fig. 3A). The DE and floodplain sediments

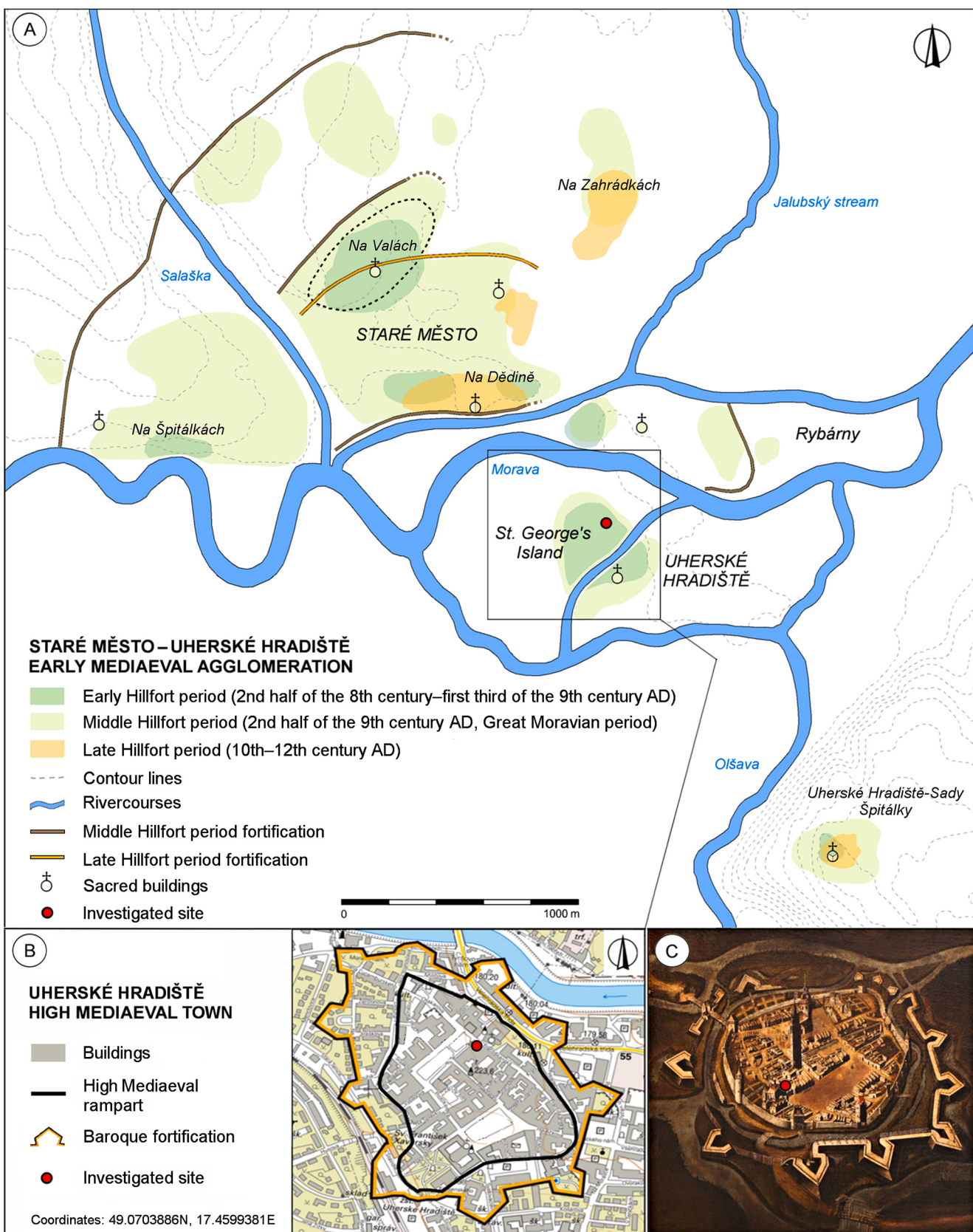


Fig. 2. A – Range of settlement areas in Staré Město and Uherské Hradiště and its vicinity from the Early to Late Hillfort period. B – Location of the site within the scope of the High Mediaeval town and the baroque fortress. C – Investigated area on the 1670 town veduta.

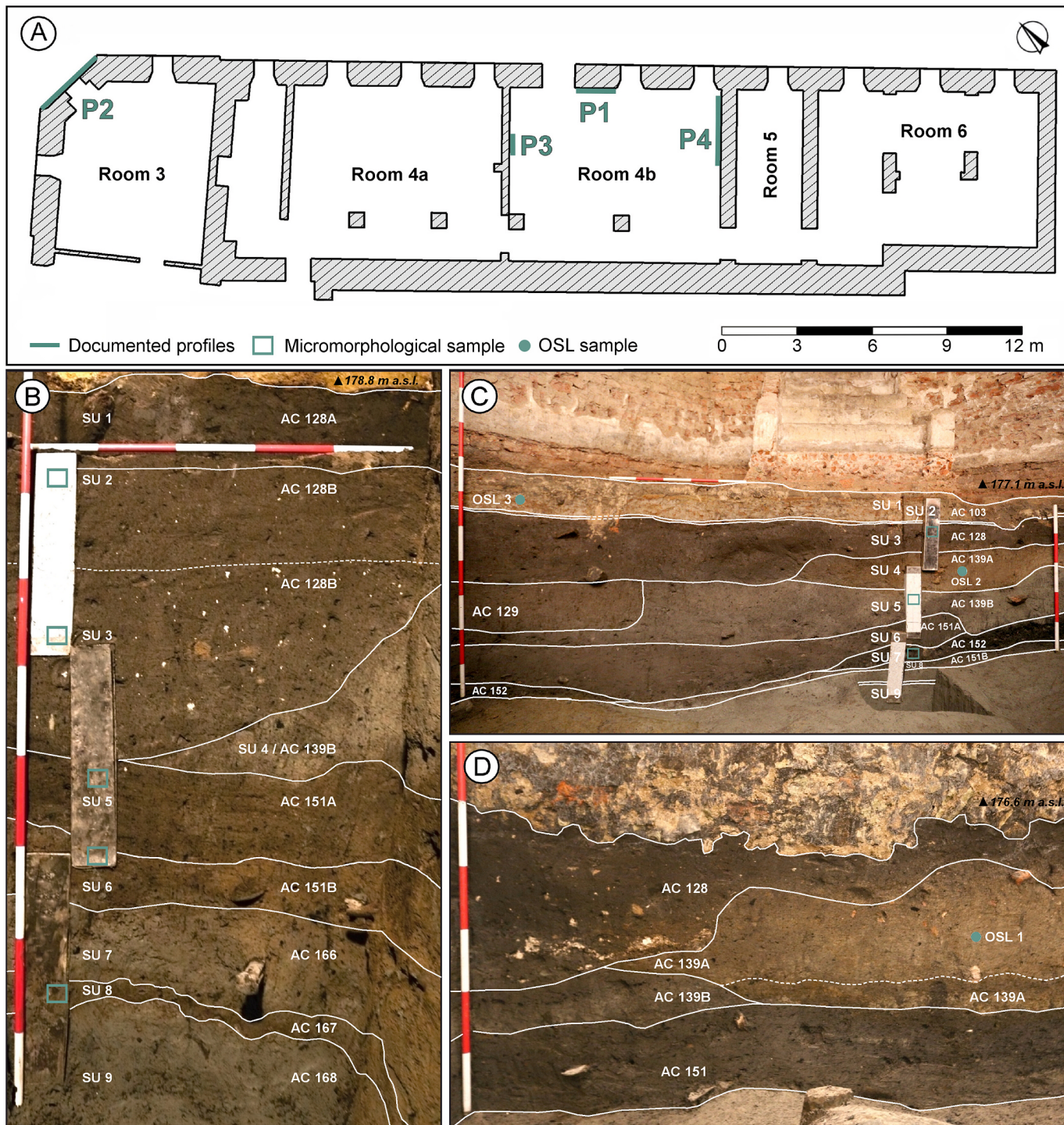


Fig. 3. A – Plan of part of the investigated area divided into rooms, with the position of studied sections marked as P1–P4. B – P1 located in the river channel in Room 4b with the position of collected micromorphological samples from Dark Earths. C – P2 located on the riverbank in Room 3 with the position of collected micromorphological samples from Dark Earths and overbank deposits, as well as samples for optically stimulated luminescence dating. D – P4 located in the river channel in Room 4b with the position of sample for optically stimulated luminescence dating. Noteworthy is the significant accumulation of fragments of lime mortar and plaster concentrated at the base of context 128.

were examined in three sections (P1–P3) in rooms 3, 4a and 4b (Fig. 3 and Fig. 4). A basic macroscopic soil and sedimentary description was performed in the field following guidelines for soil profile description (Čurlík and Šurina 1998; FAO, 2006).

3.2. Soil micromorphology and μ XRF mapping of thin sections

Nine undisturbed samples (five from P1, three from P2 and one from P3) were collected in Kubiëna tins. Preparation of thin sections followed standard laboratory procedures (Murphy, 1986). The thin sections were analysed under a polarising microscope in transmitted polarised light (PPL) and under crossed polarised light (XPL) at a magnification of ca.

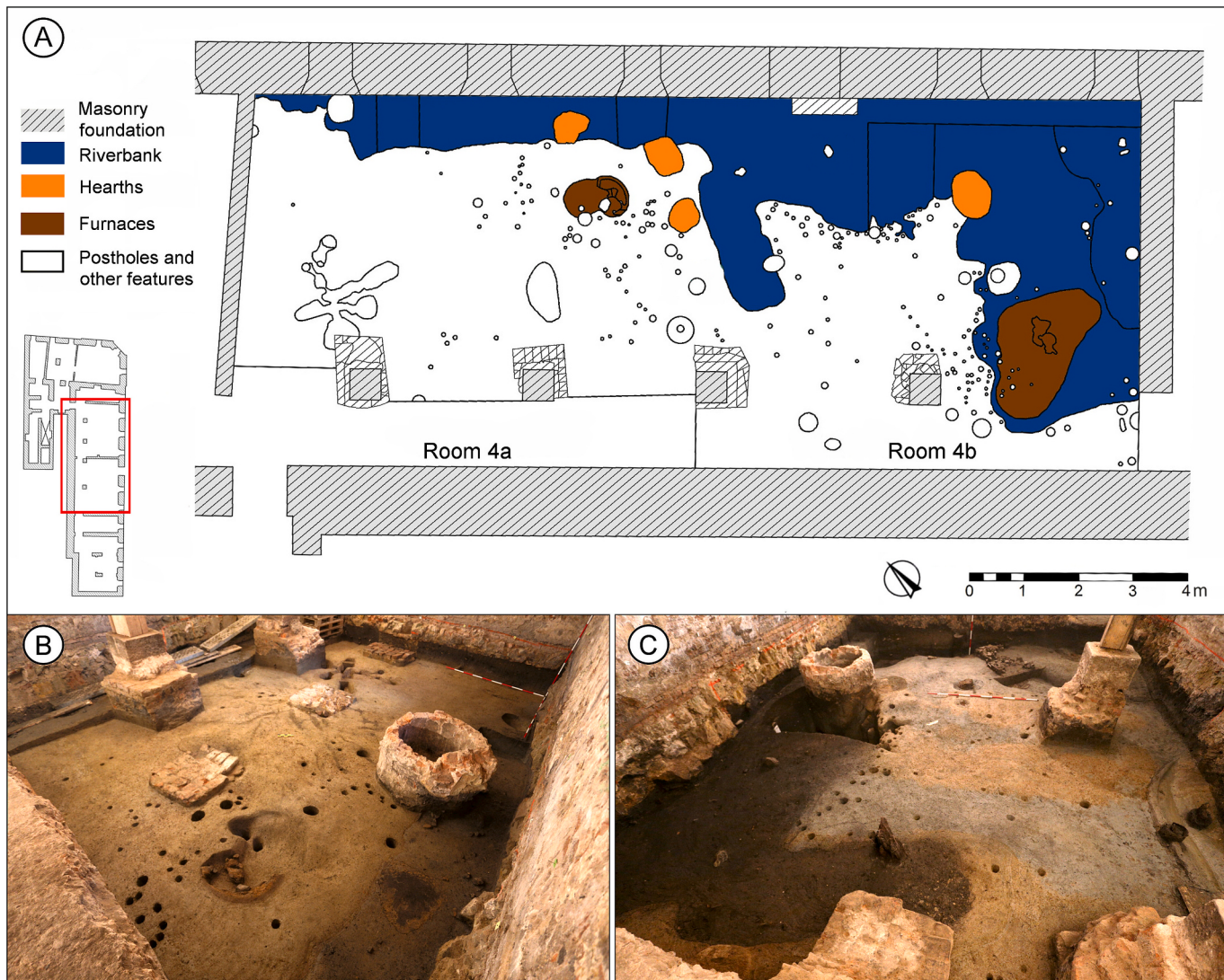


Fig. 4. A – Planigraphy of the excavation in Rooms 4a and 4b with reconstruction of the channel bank (blue) and positions of open hearths (orange), furnaces (brown), and numerous post and stake holes from above-ground structures. Most of the sunken features can be associated with settlement activities from the second half of the 8th century. Some of the postholes (especially those sunk into the buried riverbank) may date back to the 9th century or possibly belong to the earliest High Mediaeval settlement. B – View of the excavated area in Room 4a. C – View of the excavated area in Room 4b.

40–400×, following standard guidelines (Bullock et al., 1985; Stoops, 2021). The thin sections were also scanned on an EPSON Scan at 3200 ppi resolution in PPL.

The elemental composition of the nine thin section surfaces was mapped using the micro X-ray fluorescence (μ XRF) spectrometer Atlas X 8010 (IXRF, USA) equipped with a 50 w (50 kV, 1 mA) X-ray tube with an Rh anode, polycapillary focusing optics with top-down perpendicular geometry and semiconductor silicon drift detector with resolution \leq 130 eV. The X-ray tube was operated at a voltage of 20 kV and current of 500 A. Samples were analyzed in a vacuum with a spatial resolution of 50 μ m and an integration time of 100 mS. Data were processed using Iridium Ultra software.

3.3. Physico-chemical analyses

The particle size distribution of individual stratigraphical units (SU) in P1 and P2 was determined using a Bettersizer S3 Plus instrument combining laser and optical granulometry. A total of 18 samples were chemically pre-treated by dispersing them in distilled water with sodium hexametaphosphate to prevent particle flocculation. The limits of basic size fraction categories are following: clay (up to 3.9 μ m), silt (3.9–63

μ m) and sand (63–2000 μ m) according to Wentworth (1922). Similarity indices (Comparative Particle Size Distribution index matrices, hereafter: S.I.) were calculated following Langohr et al. (1976). Mass-specific magnetic susceptibility (χ) was measured on 64 samples from P1 and P2 using an Agico Kappabridge MFK1-FA device set at a frequency of 976 Hz operating with a magnetic field amplitude of 200 A/m. Data were normalised using the mass of each sample on mass-specific magnetic susceptibility (χ_{mass}) using the following equation: $\chi_{\text{f1}}/\text{mass} \times 100$ (expressed in $\text{m}^3 \text{kg}^{-1}$). The chemical composition was determined on the same samples using a Rigaku NexCG energy dispersive X-ray fluorescence spectrometer with a 50-W Pd tube with an SSD detector of 145-eV resolution (for detail see Adamová and Petřík, 2022).

3.4. Dating methods

The OSL dating of three samples was performed at the Scientific-Didactic Laboratory Centre of the Institute of Geography of Jan Kochanowski University in Kielce, Poland. For the purpose of uranium, thorium and potassium concentration value measurement, a Natural Radionuclide Analyser ‘Mazar-01’ was used. Cosmic radiation influence was considered while calculating the annual dose rate (in Gy/Ka).

Table 1

Lithostratigraphic description of the studied Profiles (=P) and stratigraphic units (=SU), modeled geochronology (68.3 % probability), archeological context (=AC), archaeological findings (AF) and interpretations.

SU	Depth [cm]	Description	Dating (AD)	Interpretation
Profile 1				
SU 1	250–290	Blackish brown silty loam with a diffuse boundary downwards; INC: charcoal, fragments of pottery, animal bones and daub, occasionally mortar; AC: 128A	850–940 (hiatus to 1240)	Organo-mineral surface horizon buried by Modern period construction material
SU 2	290–310	Dark blackish brown silty loam with a diffuse boundary downwards; INC: charcoal, fragments of pottery, animal bones and daub, occasionally mortar; AC: 128B		Organo-mineral surface horizon, open space
SU 3	310–358	Dark blackish brown silty loam to loam with a diffuse boundary downwards; INC: charcoal, stone fragments (up to 5 cm), pottery, bones and fine fragments of daub and mortars (up to 0.5 cm), antler artefacts, iron artefacts; AC: 128B	820–880	Intentional backfilling of the channel, possible levelling of terrain
SU 4	358–360	Grey silty loam with an abrupt boundary downwards; INC: charcoal, fragments of pottery and animal bones; AC: 139B	790–850	Alluvial deposits
SU 5	360–380	Brownish grey silt loam with a diffuse boundary downwards; INC: charcoal, stones (up to 15 cm), pottery and animal bones, daub, whetstone, iron artefacts, slag; AC: 151A	760–820	Organo-mineral surface horizon, intensively trampled, open space
SU 6	380–400	Brown silty loam with a diffuse boundary downwards; INC: pottery fragments, animal bones, daub, small stones; AC: 151B		Disturbed organo-mineral surface horizon, open space
SU 7	400–410	Grey clayey silty loam with a sharp undulating transition downwards; INC: isolated animal bones; AC: 166		Fluvial deposits
SU 8	410–423	Brown fine silty loam with an abrupt wavy boundary following the inclination towards the channel; INC: rare charcoal and fragments of bone; AC: 167 without artefacts	670–740	Organo-mineral surface horizon, intensively trampled, open space
SU 9	423–670	Dark grey silty loam with layer of charcoal in upper part; INC: charcoal; AC: 168 without artefacts	540–620	Overbank deposits
SU 10	>670	Sand with fragments of wood		Fluvial deposits
Profile 2				
SU 1	260–278	Alternating layers of grey and brown silty-clay loam with sharp boundary downwards; INC: pottery fragments, animal bones, bone artefact, fragment of a glass goblet, small stones; AC: 103	1260–1330	Crevasse-splay buried by Modern period construction material
SU 2	278–280	Yellowish pale grey silt; AC: 105 without artefacts	Before 1260	Mediaeval floor
SU 3	280–300	Dark blackish brown sandy loam; INC: stones and small fragments of mortar, daub, pottery fragments, animal bones, iron artefacts, small stones; AC: 128	820–940	Organo-mineral surface horizon, trampled, open space
SU 4	300–325	Brownish grey loam; INC: charcoal, pottery fragments, animal bones, mortar, daub, stones; AC: 139A	790–850	Overbank deposits
SU 5	325–340	Grey silty loam; INC: charcoal, pottery fragments, animal bones, mortar, daub, small stones; AC: 139B		Overbank deposits
SU 6	340–360	Grey silty loam; INC: charcoal, stones, pottery fragments, animal bones, daub, iron artefacts, whorl; AC: 151A	670–820	Organo-mineral surface horizon, intensively trampled, open space
SU 7	360–370	Dark grey to black silty loam; INC: charcoal, charred material, pottery fragments, animal bones, daub; AC: 152		Dump, possibly raising of the terrain
SU 8	370–380	Dark grey to black silty loam; INC: charcoal, pottery fragments, animal bones, daub; AC: 151B		Organo-mineral surface horizon
SU 9	>380	Dark grey silty loam with layer of charcoal in upper part; INC: charcoal; AC: 168 without artefacts	540–620	Overbank deposits
Profile 3				
SU 1	260–267	Yellowish pale grey silt; AC: 105 without artefacts	Before 1253	Mediaeval floor buried by Modern period construction material
SU 2	267–290	Blackish brown silty loam; INC: pottery fragments, animal bones, mortar, iron artefacts, small stones; AC: 128	850–940	Organo-mineral surface horizon, trampled, open space
SU 3	290–305	Brownish grey silty loam; INC: fragments of pottery and animal bones; AC: 139	790–850	Overbank deposits
SU 4	305–320	Grey medium silty loam; INC: pottery fragments, animal bones, daub, iron artefacts, small stones; AC: 151	670–820	Organo-mineral surface horizon, open space, intensively trampled
SU 5	>320	Dark grey sandy silty loam; INC: charcoal horizon; AC: 168 without artefacts	540–620	Overbank deposits

Samples were treated with 10 % HCl, 40 % HF and H₂O₂ to remove carbonates and organic materials. They were then sieved to 63–210 µm. Density separation was performed using SPT diluted to standard densities to isolate heavy mineral (>2.70 g cm⁻³) and quartz mineral grains (2.70–2.62 g cm⁻³). The OSL measurement was conducted using a Manual Reader-Analyser TL/OSL RA'04. A part of the fraction of each sample was irradiated with doses of 100, 200 and 300 (Gy/Ka). Quartz portions (0.5 mg) were stimulated with 470-nm blue light and an equivalent dose (ED) was calculated using the regeneration method (Murray and Wintle, 2000). The OSL age was calculated dividing the ED by the annual dose rate with measurement error of ± 15 %. Radiocarbon dating of four charcoal fragments and two charred cereal grains was performed at the Department of Earth System Science of the University of California, Irvine (lab. code UCIAMS). Samples were pre-treated according to standard protocols using HCl and HCl-NaOH-HCl (Santos et al., 2007). All results were corrected for isotopic fractionation according to the conventions reported by Stuiver and Polach (1977), with d₁₃C values measured on prepared graphite using an AMS spectrometer.

Five stakes were processed in the Laboratory of Dendrochronology of the Department of Wood Science of Mendel University in Brno according to a standard dendrochronological methodology (Cook and Kairiukstis, 1990; Rybníček, 2004). The tree-ring sequences of the samples were measured. An average tree-ring curve was created from the tree-ring curves, which were dated according to the Moravian oak standard chronology (Prokop et al., 2017).

The proposed chronostratigraphic model developed using Bayesian modelling, is based on 14C, OSL, dendrochronological ages, and a coin. The Bayesian model was constructed in OxCal 4.4. The 14C ages were calibrated using the IntCal20 calibration curve (Reimer et al., 2020) and expressed in thousands of calendar years before the present (cal BP). Individual dates were grouped into phases, for which an OxCal outlier analysis was performed (Bronk Ramsey, 2009). For each phase, a summarised age (mean and standard deviation) (Bronk Ramsey, 2017) was calculated. The modelled values (68.3 % probabilities) of ‘boundary start from’ and ‘boundary end to’ were rounded to the nearest dozen to express the time range of the individual phases/units.

3.5. Palaeobotanical analysis

Pollen samples were processed using the standard method of acetolysis using hydrofluoric acid (Moore et al., 1991). Approximately 1 cm³ of sediment per sample was used to obtain pollen extracts, identified using palynological atlases (Beug, 2004; Moore et al., 1991). The pollen diagram was created using the POLPAL program (Nalepka and Walanusz, 2003). Each sample contained at least 300 pollen grains, with *Alnus* and Cyperaceae excluded from the terrestrial pollen sum. Pollen was preserved only at the base of P1 (426–386 cm depth), while other samples contained only microcharcoal and isolated pollen grains.

Charcoals and macro-remains were obtained by water flotation (volume of ca. 5 l of each sample), followed by wet sieving using a 200-µm diameter mesh (Jacomet and Kreuz, 1999). Charcoal analysis was performed only on fragments larger than 2 mm, which were identified using an episcopic microscope with 50–200 × magnification and a reference collection (Schweingruber, 1990). The macro-remains were dried, examined under an Olympus dissecting microscope (magnifications of 12 × and greater) and identified according to standard literature (Cappers et al., 2012) and a reference collection.

4. Results

Field descriptions can be found in Table 1. Micromorphological data are summarized in Table 2. The µXRF-images (Fig. 5) show that the visible charcoal particles in SU 8 are typically enriched with P and Ca, while the soil matrix appears to be rather poor in P. Although some charcoal particles also show this relation in SUs 6 and 5, the link is less systematic. For SU 4, however, P together with Ca is also present within

the soil matrix. All three SUs contain indicates the simultaneous presence of Fe and S, which likely suggests the formation of iron sulfates. SU 2, finally shows the combined presence of Fe and S, probably indicating iron-sulphates. Physico-chemical results are presented in Fig. 6, Table 3 and Supplementary material (SM) 1. In general, silt fraction prevails in both profiles. SI (Fig. 7) show very high (above 90 %) and high (above 85 %) probabilities in P1, while in P2, mostly low values (below 85 %) are present. Table 4, Fig. 8. And SM 2 report dating results. The palaeoecological data can be found in Fig. 6 and the SM 3. The data is also available on the Zenodo platform (Adameková et al., 2025).

The studied sediments consist of fluvial and alluvial deposits alternating with the sequence of DEs and floors, dating from approximately the 6th to 14th centuries AD. Stratigraphic differences between the profiles are due to their distinct geomorphological settings. P1 is located in the depression of an ancient water channel, while P2 is on the bank of this channel documented along most of the northern edge of the excavated area. P3 documents more or less the central (highest) part of the area (Fig. 3A). Importantly, some SU can be correlated, which allows us to create a comprehensive and general picture of the site development from the proto-urban environment to the emergence of the mediaeval city of Uherské Hradiště.

5. Discussion

5.1. Taphonomy

Whereas for most part of the sequence bioturbation is limited, this is not the case for the DE's. Within them ubiquitous signs of homogenisation of the sedimentary matrix can be observed, including channels, passage features and biospheroids.

Generally, in the lower part of the studied profiles, we observed secondary formed ferrous iron phosphate minerals (vivianites) and iron sulphide minerals (pyrites) (Table 2), indicating prevailing reducing conditions (Huisman et al., 2009; Karkanas et al., 2010), hence suggesting an excellent preservation of organic remains. Few ferruginous pedofeatures (mainly orthic Fe nodules) were present in the upper part, indicating short episodes of water saturation or a rapid fluctuation of the water table (Rabenhorst et al., 1998; Karkanas et al., 2010; Lindbo et al., 2010). Their presence suggests a poorer organic preservation for these units (see further).

5.2. Reconstruction of depository history: Holocene fluvial and alluvial deposits

The bottom part of the studied area is formed by sand (SU 10) of unknown origin and age. These deposits were covered by overbank deposits (SU 9) formed by aggradation of the Morava River lasting until the Early Mediaeval Ages (transition of the 6th and 7th centuries AD) as it was proved by dating of a charcoal layer (Table 4, Fig. 8). Except for the charcoal layer reflecting one of the first human activities on the island of St. George, the sediments bring no evidence of direct anthropogenic activity. Similarly, the pollen record (Fig. 6B) indicates a forested alluvium only weakly impacted by humans as shown by the limited amount of indicators of human presence such as cereals and ruderal species e.g. *Artemisia* or *Chenopodiaceae*. Woodland compositions are dominated by *Quercus*, *Pinus*, *Picea*, *Abies* and less common are other trees such as *Betula*, *Fagus*, *Corylus* and *Carpinus*. Previous observations performed on sections situated ca. 150 m from the present study area also showed the presence of forested alluvium, albeit with a higher abundance of wetland willow (*Salix*) and alder (*Alnus*) (see Svitavská-Svobodová, 2011). While the possibility of long-distance transport of pollen or charcoal in alluvial sediments should be considered (Hall and Huntley, 2007), many of the identified species are likely representative of the nearby vegetation (Opravil, 1984; 1985; 1999).

Such an extensive (thickness of ca. 150 cm) aggradation of overbank deposits, dated before 540 CE, has not yet been identified in the

Table 2

Results of micromorphological observation of selected stratigraphic units (=SU) from studied profiles (P). The terminology is modified after [Stoops \(2021\)](#). The classification is as follows: present (P) = <1%, very few (VF) = 2–5 %, few (F) = 5–15 %, common (C) = 15–30 %, frequent (F) = 30–50 %.

SU/ Profile	Microstructure and voids	Groundmass c/f distri- bution	Fine fraction	Coarse fraction	Organic material	Anthropogenic inclusions	Inorganic residues of biological origin	Pedofeatures
SU 2P1	Subangular blocky; Channels, planes, complex packing	Porphyric	Dark brown, undifferentiated	Unsorted silt, quartz, feldspar, micas, glaucite, fragments of rocks	Fine material (FR), plant tissue (P), roots (P), fungi spores (P), seed coats (P)	Charcoals (VF), burned (P) and unburned (VF) bones, earth construction material (VF), metal slag (VF), coprolites (P), parasite eggs (P), wood (P)	Isolated phytoliths (P), diatoms (P)	Dusty clay coating (P), clay coating (P), Fe/Mn pedofeatures (P), phosphatic nodules (P), biospheroids (P)
SU 3P1	Granular to poorly develop subangular blocky; Planes, complex packing, vughs, channels	Porphyric	Brown, striated and undifferentiated	Unsorted silt; quartz, feldspar, micas, glaucite, fragments of rocks	Fine material (FR), plant tissue (P), roots (P), fungi spores (P), seed coats (P)	Charcoals (F), burned (P) and unburned (P) bones, earth construction material (VF), coprolites (P), mortar (P), metal slag (P), daub (P), wood (P)	Shell fragments (P), isolated phytoliths (P), sponge spicule (P)	Dusty clay coating (P), passage features (P), phosphatic nodules (P), Fe/Mn nodules (P), vivianite infillings, crystals and nodules (VF)
SU 5P1	Upper part: Subangular blocky; Planes, channels Lower part: Platypic; Chambers, complex packing voids, planes	Porphyric	Brown to dark brown, undifferentiated, locally striated	Unsorted silt; quartz, feldspar, micas, glaucite, fragments of rocks	Fine material (FR), plant tissue (FR), roots (P), fungi spores (P), seed coats (P)	Charcoals (F), burned (P) and unburned (P) bones, earth construction material (P), ashes (P), metal slag and glass-like silica (P), coprolites (P), parasite eggs (P), wood (P), charred material (C)	Articulated and isolated phytoliths (VF)	Fe/Mn nodules (P), phosphatic nodules (P), Ca nodules (P), vivianite infillings, crystals and nodules (F), passage features (P), dusty coating (P)
SU 6P1	Subangular blocky; Planes, channels	Porphyric	Brown, undifferentiated, locally crystallitic, porosetrated	Moderately sorted silt; quartz, feldspar, micas, glaucite, fragments of rocks	Fine material (FR), plant tissue (FR), roots (P), fungi spores (P)	Charcoals (F), burned (P) and unburned (P) bones, earth construction material (P), ashes (VF), coprolites (P), parasite eggs (P), metal slag (P), charred material (VF)	Mostly isolated phytoliths (P), shell (P)	Dusty clay coating (P), passage features (P), Fe/Mn nodules (P), vivianite infillings, crystals and nodules (C)
SU 8P1	Angular to subangular; Planes and rare chambers and vughs	Porphyric	Brown to reddish brown, undifferentiated	Poorly sorted silt with occasional intrusion of sand; quartz, feldspar, micas, glaucite, fragments of rocks	Fine material (FR), plant tissue (FR), roots (P), fungi spores (P), seed coats (P)	Charcoals (VF), burned (P) and unburned (P) bones, earth construction material (P), metal slag (P)	Phytoliths mostly isolated (P)	Passage features (C), vivianite infillings, crystals and nodules (C), Fe/Mn nodules (P)
SU 3P2	Granular, locally single grain; Planes and channels	Porphyric	Brown, undifferentiated, locally porosetrated, granostrated	Poorly sorted to unsorted silty sand; quartz, feldspar, micas, fragments of rocks	Fine material (F), plant tissue (P), roots (P)	Charcoals (VF), unburned bones (P), earth construction material (P), ashes (P)	Isolated phytoliths (P)	Passage features (P), phosphatic nodules and coatings (F), Fe/ Mn nodules (P), dusty infilling (VF)
SU 5P2	Single grain	Porphyric	Brown, undifferentiated, locally porosetrated, granostrated	Unsorted silt; quartz feldspar, micas, fragments of rocks	Fine material (F), plant tissue (P), roots (P)	Charcoals (F), unburned bones (P), ashes (P), coprolites (P)	Fragment of shell (P), isolated phytoliths (P)	Vivianite nodules, crystals and infillings (VF)
SU 7P2	Subangular blocky; Planes, complex packing voids, channels, chambers	Porphyric	Dark brown to black; undifferentiated, locally crystallitic	Unsorted silt; quartz feldspar, micas, fragments of rocks	Fine material (P), plant tissue (P), roots (P), fungi spores (P),	Charcoals (C), burned (P) and unburned (F) bones, earth construction material (P), burned mortar (P), ashes (VF), coprolites (P), ashes (P), charred material (C)	Fragment of shell (P), isolated phytoliths (P)	Vivianite nodules, crystals and infillings (VF), passage features (P)
SU 2P3	Subangular to angular blocky; Planes and channels	Porphyric	Brown, undifferentiated, locally porosetrated, granostrated	Unsorted to poorly sorted silty sandy, quartz feldspar, micas, fragments of rocks	Fine material (F), plant tissue (P), roots (P)	Charcoals (VF), burned (P) and unburned (P) bones (P), earth construction material (P), coprolites (P)	Isolated phytoliths (P)	Passage features (P), phosphatic nodules and coatings (F), dusty infilling (VF)

catchment of the Morava River (cf. [Kadlec et al., 2009](#); [Kadlec et al., 2022](#)). In fact, the earliest phase of aggradation of the Morava River was documented after 700 CE and situated approximately 20 km south of the studied location, in the area of Strážnice ([Grygar et al., 2011](#)).

5.3. Dark Earth formation processes

5.3.1. Early Mediaeval Ages: Early Hillfort period (late 7th–8th century CE)

The oldest Dark Earth (SU 8, P1) developed from the late 7th century to the early 8th century CE within fluvial deposits mixed with anthropogenic components ([Fig. 5A](#)). During the formation of this DE there was

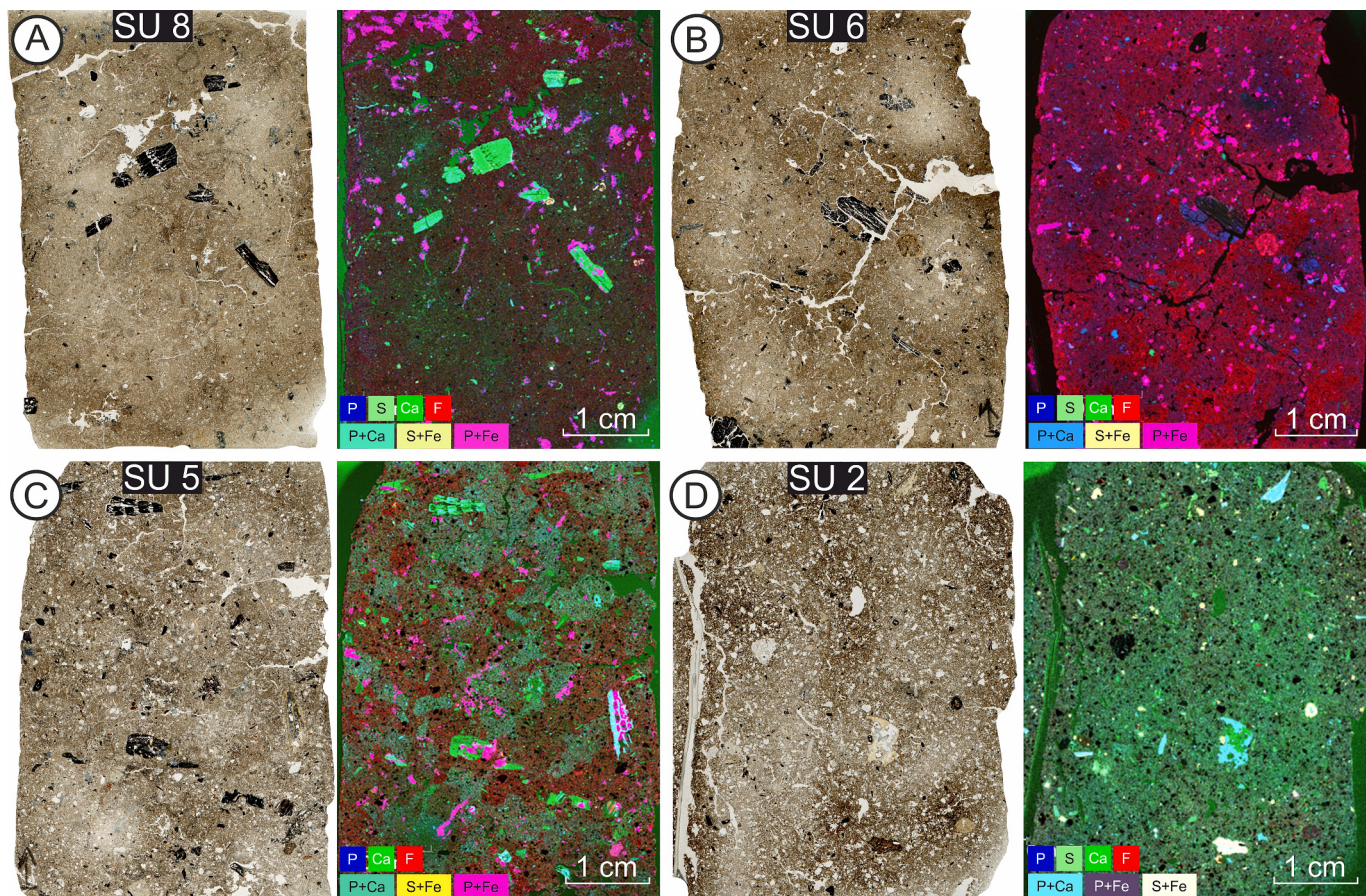


Fig. 5. The figure presents paired images of thin section scans (left) and corresponding μ XRF element distribution maps (right) for four selected stratigraphic units: (A) SU 8, (B) SU 6, (C) SU 5, and (D) SU 2. The thin section scans reveal microstructural and sedimentary features, such as organic inclusions and anthropogenic materials. The μ XRF maps highlight the spatial distribution of key elements, including phosphorus (P), sulfur (S), calcium (Ca), and iron (Fe), coded in different colors. The element associations should illustrate the following: P + Ca = bone fragments, S + Fe = fragments of slag, P + Fe = vivianite.

no permanent standing water in the channel, as intensive bioturbation was observed. Evidence for the bioturbation includes bow-like passage features (Fig. 5A), channel walls coated with fine organic-rich soil material (Fig. 10a) and humus enrichment (Kooistra et al., 2010). This DE thus therefore corresponds to an incipient organo-mineral surface A horizon (e.g. Gerasimova et al., 2018) representing the oldest known soil formation on the island. Although this DE contains the least anthropogenic material compared to other studied DEs at the site (Fig. 9); it includes materials of various origins, such as domestic waste (burned and unburned bone fragments, Fig. 10b), earthen-based construction material and fragments of slag (Fig. 10c), the latter probably associated with craftworking in the vicinity. At least part of these components may have entered the soil through poaching (Fig. 10d), as evidenced by convolution (Rentzel et al., 2017) of the boundary between the overbank deposits and the DE (Fig. 3B). The relatively low P content (SM 1) could reflect the relatively low intensity of human activities compared to the overlying SU, as high P concentrations are often considered an indicator of ancient human activities (e.g., Devos, 2018 and references therein).

At the same time, the basal DE (SU 8, P2), formed on overbank deposits (SU 9) with high anthropogenic input (peaks of P and Ca), developed on the riverbank in the northwest corner. It was later buried by another DE (SU 7), likely a homogeneous dump of domestic waste including up to 60 % charred material, ceramics, ashes, bones, and shell fragments (Fig. 10e, f). Relatively high P and Ca values in P2 (Fig. 6A, SM 1) could be linked with decomposing bones and ashes. This dump was possibly to raise the terrain to protect it against flooding (cf. Nicosia et al., 2012). In the central area (P3), a thick DE (SU 4) formed on the overbank deposits, but due to the lack of dating, its correlation with

lower DEs in P1 and P2 remains hypothetical (Fig. 6A).

The period of soil formation in the channel was followed by a reactivation of the channel at the beginning of the 8th century CE (Fig. 8) during which a thick layer of silty loam (SU 7) was deposited (Fig. 3B). Neither can be ruled out, intentional or natural re-activation. As no alluvial sediments were observed elsewhere, the water probably did not spill out of the channel.

This is followed by the formation of another DE (SU 6) dated to the 8th century CE (Fig. 8). It developed from fluvial deposits mixed with anthropogenic components (Fig. 5B). Sediments comes probably from another re-activation that deposited very similar material to those of SU 5 (Fig. 7). The DE represents the formation of another ancient A horizon (Gerasimova et al., 2018) in the ancient channel, which means that water was not present for a certain period. Intensive bioturbation and the relatively elevated decomposed organic matter (humus) content indicates a higher degree of maturity and longer or more intense development of the DE compared with the underlying DE (SU 8). Again, at least a part of the anthropogenic components probably entered also through poaching (Rentzel et al., 2017). In this respect we can also refer to the presence of dusty clay coatings possibly related to disturbed surfaces (Courty et al., 1989; Macphail et al., 1990). The increasing abundance of randomly distributed anthropogenic components also indicates a stronger degree of anthropisation which is also reflected by increased P and Ca contents (e.g. Holliday and Gartner, 2007; Cook et al., 2014) (Fig. 6A). The combined presence of charcoal and ashes (Fig. 10g), charred black material, burned and unburned bones and shell fragments points to household waste (Devos et al., 2009; 2022). The observed vitrified ash indicates high temperature heating and together

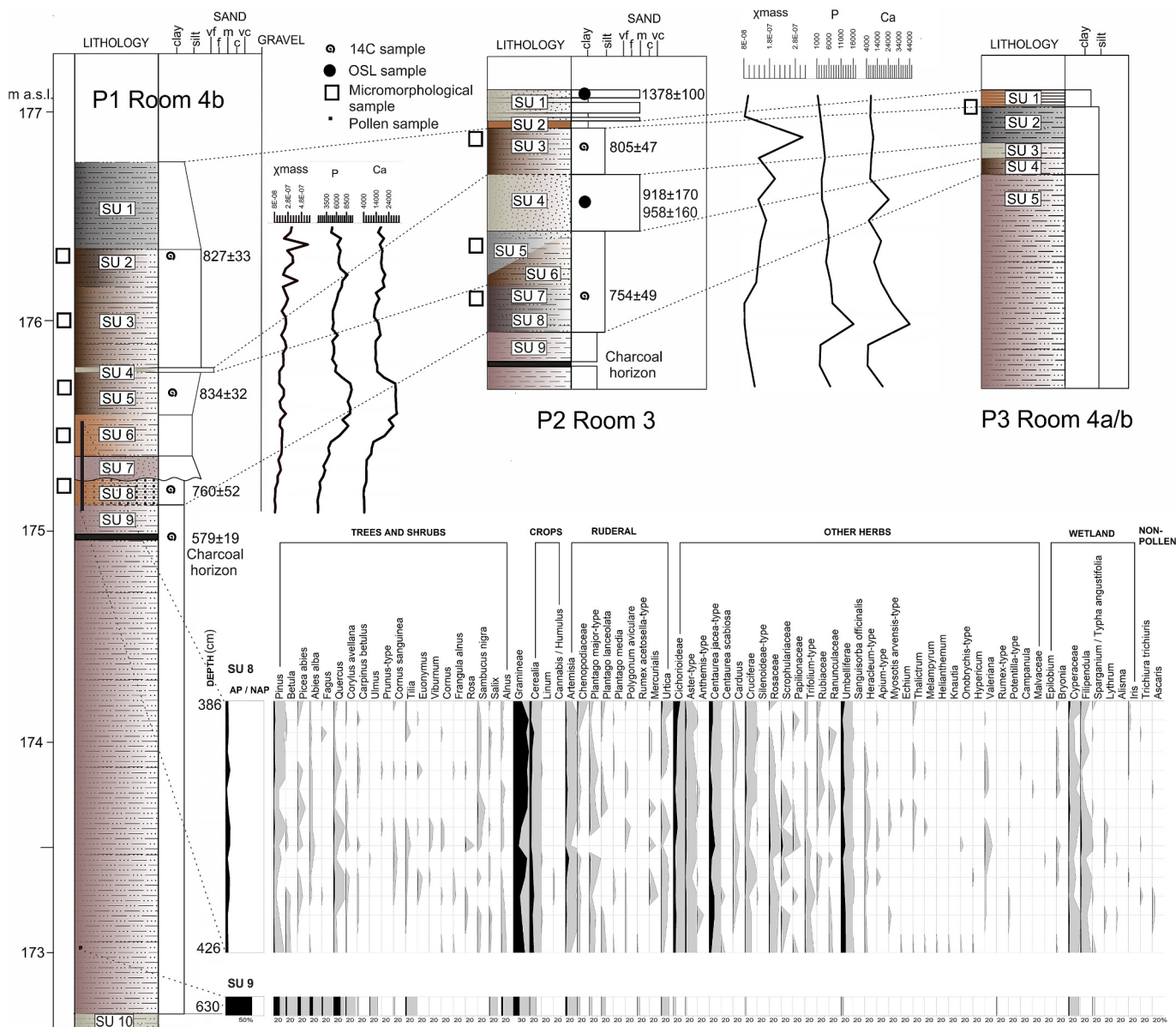


Fig. 6. A – Idealized correlation between studied profiles P1, P2, and P3 in Room 3, Room 4a, and Room 4b at the Uherské Hradiště site with grain-size distribution, and geochemical data (e.g., Ca content). Radiocarbon ($14C = \mu \pm \sigma$ cal. BC/AD), optically stimulated luminescence (OSL), micromorphological, and pollen samples are marked at respective depths. B – Palynological percentage diagram of selected taxa of P1 from the depth of 426–386 cm (SU 9 and 8) dated to the 8th century CE (Early Hillfort period).

with the, albeit rare, fragments of slag it reveals the presence of metallurgical/artisanal waste. Besides, excremental waste (Fig. 10h) including parasite eggs of *Ascaris* and *Trichuris* and construction waste (earthen based construction material) have also been observed. According to macroscopic characteristics and stratigraphic position, the SU 6 on the riverbank (P2) can be correlated with SU 6 and/or SU 5 formed in the channel (P1) and therefore probably also represent ancient surface horizon or its remains.

The following DE (SU 5) observed in the channel and dated between 760 and 820 CE (Fig. 8, SM 2) was also interpreted as a surface organo-mineral A horizon that was disturbed by walking. It is evidenced by signs of bioturbation as well as convolution (Fig. 10i) and fragmented charcoals (Rentzel et al., 2017; Karkanas et al., 2010). The formation is very similar to the previous DE (SU 6) in the ancient channel and the fluvial parent material was probably deposited during re-activation of the channel. The quantity of anthropogenic components, such as excremental waste, kitchen waste (Fig. 10j), metallurgical waste (Fig. 10k)

and construction material increase (Fig. 9) as well as the P and Ca contents (Fig. 6A). This DE contains a visibly larger amount of charred black material (Fig. 10l).

Above this DE, we observed a thick layer of silty loam (SU 4) that could indicate a short-term recovery of water activity in the channel, which must according to field observations already have been very shallow at the edge of 8th and 9th century CE. In other parts of the site (P2 and P3), we also observed sediment of alluvial origin, which, according to dating and stratigraphy, could be deposited at approximately the same time: overbank deposits (SU 5) in P2 containing anthropogenic materials (Fig. 11a) and overbank deposits (SU 3) in P3.

The preserved pollen record (Fig. 6B) from the 8th century CE (SU 8–6) is valuable because we have relatively little information about this period. Natural profiles outside the Early Medieval agglomeration show extensive human impact on the floodplain of the Morava River (Placek and Dejmal, 2015). Our data reveal a deforested local environment characterized by abundant grasses and ruderal species. High

Table 3

Results of grain-size distribution of Profile 1 and 2. The size fractions were divided into several categories: clay (up to 3.9 µm), very fine silt (3.9–7.8 µm), fine silt (7.8–15.6 µm), medium silt (15.6–31 µm), coarse silt (31–63 µm), very fine sand (63–125 µm), fine sand (125–250 µm) and medium sand (250–500 µm) according to Wentworth (1922).

Depth [cm]	SU	Clay	Very fine silt	Fine silt	Medium silt	Coarse silt	Very fine sand	Fine sand	Medium sand	Coarse sand	Very coarse sand
Profile 1											
290	2	14.48	12.3	14.3	18.69	19.78	12.75	5.74	1.75	0.17	0
296	2	14.75	12.98	14.65	18.46	18.86	11.87	5.59	2.32	0.5	0
335	3	10.53	9.405	10.765	14.675	16.18	11.21	7.88	12.295	6.565	0.465
359	4	10.48	11.75	13.8	18.68	20.11	21.31	3.85	0	0	0
368	5	13.93	13.85	16.13	20	19.07	11.14	4.16	1.7	0	0
391	6	12.12	13.03	15.91	20.79	21.83	12.12	3.53	0.65	0	0
406	7	8.18	9.1	11.62	20.15	22.94	23.57	4.42	0	0	0
417	8	18.53	16.02	17.3	20.69	15.82	7.87	2.73	0.95	0.06	0
429	9	8.99	8.04	10.05	18.13	27.38	22.12	5	0.28	0	0
Profile 2											
15	1	27.71	21.25	19.08	15.5	5.57	2.31	5.31	3.1	0.14	0
25	3	7.3	6.14	7.01	9.9	11.54	9.46	11.11	20.76	15.32	1.43
65	5	15.17	13.4	14.35	19.72	20.06	16.15	1.14	0	0	0
85	6	14.22	13.35	14.96	17.84	14.72	8.62	7.09	7.76	1.42	0
105	8	24.31	13.68	15.56	19.4	17	8.12	1.7	0.2	0	0
125	9	11.59	11.13	13.39	19.17	22.62	14.93	5.57	1.57	0	0

Profile 1

Depth/SU	290-2	296-2	340-3	359-4	368-5	391-6	406-7	417-8	429-9
290-2	100	98	69	91	95	93	85	87	83
296-2		100	70	91	95	93	85	87	83
340-3			100	79	79	77	75	73	74
359-4				100	98	90	93	81	90
368-5					100	95	83	91	80
391-6						100	87	89	83
406-7							100	75	94
417-8								100	72
429-9									100

Profile 2

Depth/SU	15-1	25-3	65-5	85-6	105-8	125-9
15-1	100	47	67	74	79	66
25-3		100	52	67	52	59
65-5			100	84	89	91
85-6				100	85	84
105-8					100	82
125-9						100

Fig. 7. Similarity-indices (in %) of Profile 1 and 2. These SI-indices indicate to which extent the particle size distribution of two samples are identical. Low values indicate significant differences between samples.

percentages of *Artemisia* and *Chenopodiaceae* suggest nutrient- and nitrogen-rich conditions, while the presence of pollen from *Urtica* and *Bryonia alba* indicates the existence of wet, nutrient-rich habitats. Macro-remains (SM 3) of perennial herbaceous ruderal vegetation and scrub were also recorded (*Rubus caesius*, *Sambucus ebulus*, *Sambucus nigra*). Local wetland vegetation is composed of tall sedge species, with pollen from *Sparganium* and *Filipendula*. This environment appears to have experienced intensive trampling, as evidenced by pollen from *Plantago major* and *Polygonum aviculare*. Furthermore, the pollen of *Mercurialis annua* and macro-remains of *Potentilla cf. supina*, *Chenopodium album*, *Chenopodium hybridum*, *Chenopodium polyspermum*, and *Stachys annua* highlight disturbed soil.

The presence of cereal pollen and macro-remains of *Triticum aestivum* and *Panicum miliaceum* suggests agricultural activities and the cultivation of crops (cf. Kočár and Dreslerová, 2010). However, macro-remains of field weeds were documented only through individual finds of diaspores from common species (*Galium aparine*, *Vicia tetrasperma*) and traces of cultivation were not detected in the DEs, suggesting that crop

cultivation happened in the surroundings of the site, rather than on the site itself. A similar environment with a high abundance of anthropogenic indicators and a low percentage of cereals was recorded at the Pohansko site (Doláková et al., 2010), located approximately 55 km to the south, which later, as Uherské Hradiště, became an important Great Moravian centre (Macháček, 2010). The same picture of a deforested Early Mediaeval landscape with local ruderal vegetation and agricultural activities in pollen record was documented ca. 150 m from the studied sections (Svobodová, 1990; Svitavská-Svobodová, 2011). Moreover, Svitavská-Svobodová (2011) identified spores of *Sporormiella*, fungi that grow on cattle excrements, and pollen which indicates the presence of a water body nearby.

Quercus has been dominant in charcoal composition since the 8th century CE (SM 3). Other broadleaf trees, such as *Carpinus*, *Fraxinus*, and *Corylus*, are common components of the charcoal assemblages from this period. The presence of *Fagus* charcoal indicates its local occurrence in alluvial forests. However, it may also be interpreted as fuelwood transported from forested uplands. Similarly, *Alnus* corresponds to the

Table 4

Results of radiocarbon dating, optically stimulated luminescence (OSL) dating and dendrochronology (D). Abbreviations: UCIAMS = University of California, μ = calibrated average, σ = standard deviation, AC = archaeological context, confid. = confidence.

Lab. code	AC	Profile/ SU	Material	Result of dating (yrs. BP)	Calibrated Age (95.4 % confid.,AD)	$\mu \pm \sigma$ (cal AD)	Modelled Age (68.3 % confid.,AD)	Modelled Age (95.4 % confid.,AD)
UCIAMS-209098	128	1/2	cereal grain	14C 1210 ± 15	783–880	827 ± 33	829–866	810–875
UCIAMS-209099	151	1/5	cereal grain	14C 1200 ± 15	774–884	834 ± 32	775–808	772–831
UCIAMS-209100	167	1/8	charcoal	14C 1245 ± 20	680–876	760 ± 52	686–724	676–742
UCIAMS-217744	99	1/9	charcoal	14C 1500 ± 20	545–634	579 ± 19	565–598	546–635
UCIAMS-217745	128B	2/3	charcoal	14C 1225 ± 20	706–881	805 ± 47	862–883	839–890
UCIAMS-209102	152	2/7	charcoal	14C 1245 ± 15	682–872	754 ± 49	714–777	705–807
UH 3	103	2/1	sediment	OSL 640 ± 100		1378 ± 100	1265–1308	1259–1365
UH 2	139	2/4	sediment	OSL 1100 ± 170		918 ± 170	800–840	790–856
UH 1	139	2/4	sediment	OSL 1060 ± 160		958 ± 160	800–840	790–856
M1970	Room 6		oak	D 1260–1274	1253–1281	1267 ± 7	1256–1271	1250–1279
M1975	120		oak	D after 1211	1210–1211		1210–1211	1210–1211
M1977	118		oak	D 1222–1235	1215–1242	1228 ± 6	1224–1239	1217–1246
M1979	116		oak	D 1252–1271	1243–1277	1260 ± 8	1251–1266	1248–1274
M1980	121		oak	D 1258–1262	1256–1264	1260 ± 2	1257–1262	1255–1264

deforested alluvium identified in the pollen record. *Cornus*, an indicator of open, sunny shrub formations, is present in both the pollen and charcoal records. A similar charcoal composition was observed in Olo-mouc during the Early Mediaeval period, prior to the establishment of Great Moravia (Kočár et al., 2016).

5.3.2. Early Mediaeval Ages: Middle Hillfort period (9th and early 10th century CE)

The next development started in the channel with a DE (SU 3) formation dated between 820 and 880 CE (Fig. 8), which according to its composition, corresponds to intentional backfilling (levelling and/or dump) of the channel with waste material and building rubble mixed with silty/loamy sediments. The channel got out of function and became an open space with several generations of soil development. The backfilling was further homogenised by bioturbation reflected also in an increased MS signal (Fig. 6A). Although the Ca and P contents values are lower (SM 1), possibly related to phosphorus translocation as a result of changes in redox status (Devos et al., 2011), a strong degree of anthropisation compared with underlying DE is shown by the diversity and richness in randomly distributed anthropogenic remains. Construction/destruction debris included mortar (Fig. 11b), daub (Fig. 11c), earthen-based materials (Fig. 11d) and possibly wood (Friesem et al., 2017; Stoops et al., 2017; Macphail and Devos, 2023). Mortar fragments appear as a new building material that was used for the first time at the site probably for plastering stones, later occurring only sporadically in the upper-lying DE.

Following DE (SU 2) in P1 developed after 850 CE on flat terrain and represents another ancient organo-mineral A horizon. This interpretation based upon the presence of humus, several generations of bioturbation, an intensively developed microstructure, the presence of calcite biospheroids (Canti, 2003; 2017; Gerasimova et al., 2018) and increased MS values (Fig. 6A, SM 1) reflecting intensive pedogenesis (cf. Bloemendaal et al., 2008). The presence of dusty (dirty) coatings indicates an unprotected surface (Devos et al., 2017). The quantity of anthropogenic components including metallurgical (Fig. 11e, f), domestic, construction/destruction and excremental waste decreases

(Fig. 9), which could also indicate reducing human influence/presence. Parasite eggs indicate poor hygiene (Pichler et al., 2014; Pümpin et al., 2017; Brönnimann et al., 2020). All these components accumulated and entered to soil by trampling as proved by compaction of the sediment (Rentzel et al., 2017). It is also supported by the presence of *Polygonum arenastrum* in macroremains (SM 3), indicative of trampled surfaces.

The uppermost DE dated to the 9th century CE and later (Fig. 8) developed across the entire studied area (SU 1 in P1, SU 3 in P2, SU 2 in P3). This DE corresponds to a disturbed and trampled organo-mineral surface A horizon only weakly impacted by human activities compared with the other studied DEs (Fig. 9). Evidence for bioturbation includes few bow-like passage features (cf. Kooistra et al., 2010). This DE contains frequent phosphatic coatings and nodules and sporadic excrements (Fig. 11g–i), supported by significantly higher P content (Fig. 6A, SM 1). We found grains of wheat (*Triticum aestivum*), barley (*Hordeum vulgare*), and rye (*Secale cereale*), which could indicate the presence of crops; however, they appeared only as isolated charred remains. Similarly, field weeds like *Fallopia convolvulus* and *Galium* species were rarely documented. As such, no firm evidence for cereal cultivation on the site was found. We therefore suppose either pasture in the period when it was no longer permanently inhabited or possibly abandoned or development of wasteland or either post-depositional contamination by phosphates from upper parts of the sequence (town), for example from urban leaks that have been already observed at other sites (cf. Macphail et al., 2004; Devos et al., 2017).

Generally, the archaeobotanical analysis reveals a striking similarity in the spectrum of synanthropic species between the Early and Middle Hillfort (Great Moravia) periods, particularly the predominance of macro-remains from ruderal species like *Chenopodium* spp. and *Sambucus* spp. (SM 3). Notably, macro-remains of undemanding species such as *Cirsium arvense* and *Viola arvensis* were identified, which are commonly found in various anthropogenic habitats, including pastures and ruderal areas, dating back to the 8th century CE. A particularly notable find is the mineralized seed of *Papaver somniferum*, one of the few records from the 9th–10th centuries CE in the Czech Republic (Čech et al., 2013). Additionally, the charcoal composition (SM 3) aligns with similar Early

OxCal v4.4.4 Bronk Ramsey (2021); r:5 Atmospheric data from Reimer et al (2020)

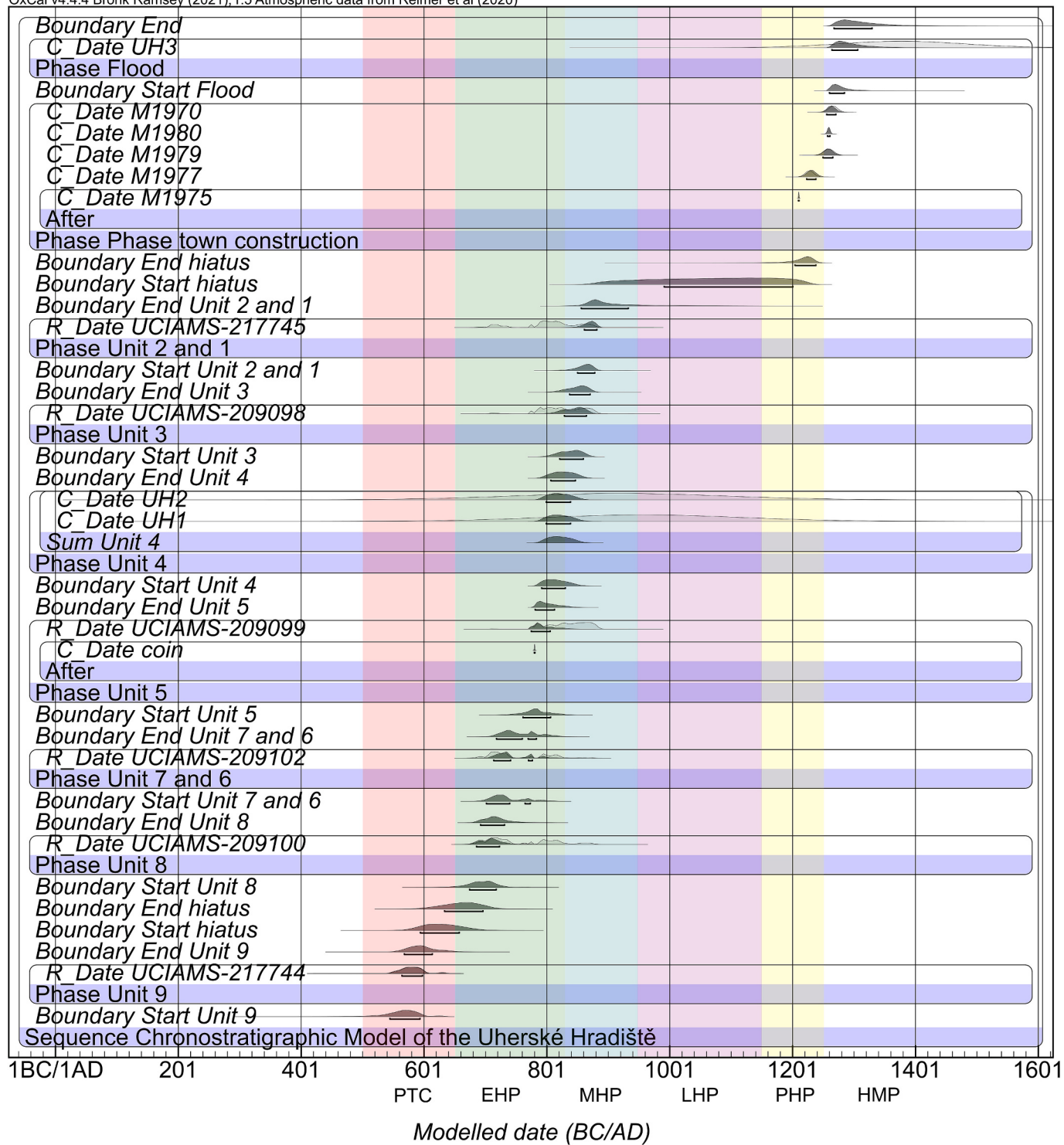


Fig. 8. Chronostratigraphic Bayesian model of the Uherské Hradiště site. The Bayesian model is composed of radiocarbon dates, OSL ages, dendrochronological ages, and coin age (calculated as “after”), ordered according to a relative age sequence of phases that represent chronological phases of sediment accumulation and soil development. Plotted are modeled and unmodeled results with 68.3 % probabilities. Abbreviations: PTC = ‘Prague-type’ culture period, EHP = Early Hillfort period, MHP = Middle Hillfort period, LHP = Late Hillfort period, PHP = Post-Hillfort period, HMP = High Mediaeval period.

Medieval sites along the Morava River, such as Přerov and Mikulčice (Procházka, 2017; Opravil, 1983), indicating continuity in building materials and fuel sources from the previous 8th-century period.

5.3.3. High Mediaeval period (from 13th century CE)

On the top of the uppermost DE, heterogeneous, microlaminated

High Mediaeval floors (Fig. 12) were preserved below younger rubble and/or building remains in some part of studied area (P2 and P3). The lowest floor surface is prepared from a 1–2 cm-thick yellowish pale grey Fe-rich loam showing Mn pedofeatures in the upper part (Fig. 12B). It is succeeded by a 1-cm-thick compacted unit rich in Ca containing calcareous ashes and charcoal (Fig. 11j, k). This layer could have formed

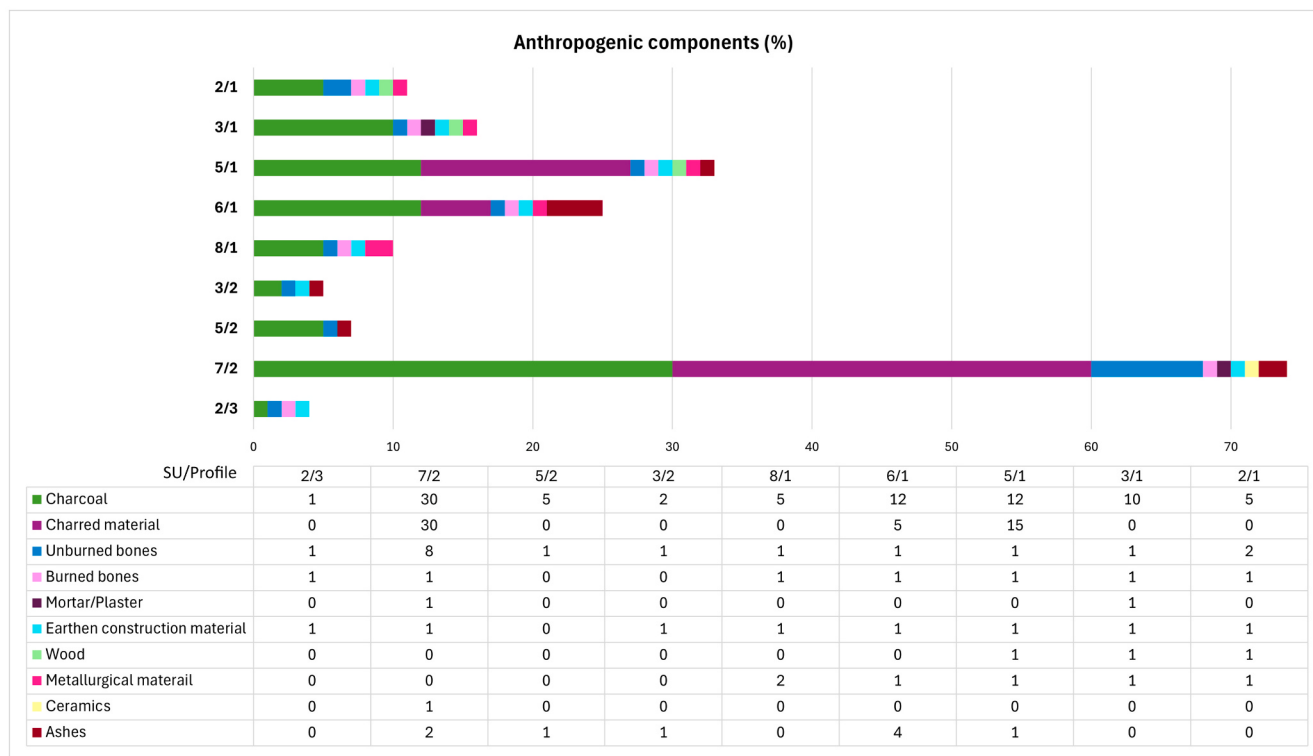


Fig. 9. The bar chart illustrates the percentage distribution of anthropogenic components, such as charcoal, charred material, burned bones, and others, identified in various stratigraphic units (SU) and profiles (e.g., 2/1, 6/2). Below the chart, a detailed table provides quantitative data for each component in each SU/profile, facilitating comparison and interpretation of anthropogenic activity in the sampled contexts.

as an accumulation of residues from domestic human activities or, particularly in case of ashes as the remnants of maintenance events (cf. Milek, 2012). Then, a 1-cm-thick layer of muddy yellowish pale grey Fe and Mn-rich material lightening upwards was accumulated corresponding to a new preparation layer, followed by another compacted Ca-rich layer containing charcoal and ashes again related to the occupation and/or maintenance of the surface (Fig. 12B). The constructed floor and the top of the DE below show a platy microstructure and planar and fissure voids, witnessing intensive trampling (cf. Gé et al., 1993; Milek, 2012; Rentzel et al., 2017) (Fig. 11). In rooms 3 and 6, the floor is buried by alluvial sediments from the turn of the 13th and 14th century CE (Fig. 8). Notably, there is a clear absence of flooding between the end of the Great Moravian settlement and the beginning of developed High Mediaeval urbanisation which probably corresponds to reduced settlement in the surrounding region. The return of regular flooding in the High Mediaeval Age continued until modern times likely resulting from intensified anthropogenic activities and significant deforestation upstream along the Morava River (cf. Kadlec et al., 2009).

The results of the archaeobotanical analysis from the High Mediaeval period are influenced by poor fossilisation conditions. Only the decay-resistant charred diaspores of synanthropic plant species (SM 3) associated with disturbed substrates and nutrient-rich areas were documented (*Chenopodium album*, *Sambucus ebulus*, *Sambucus nigra*). A nearby pollen record from Uherské Hradisté dated to 13th century CE (Svobodová, 1990) shows extremely high abundance (up to 58 %) of Cerealia (*Triticum*, *Secale*, *Hordeum* and *Avena*), which is quite typical for High Mediaeval towns (Kozáková et al., 2014). Generally, it rather demonstrates the difference between Early and High Mediaeval societies and town economies, than any environmental changes.

5.4. Interpretation of archaeological contexts integrated with geoscience insights

The discovery of a section of the extinct Morava channel represents the third find of this kind on St. George's Island. Aside from the well-known river channel ('Rechla'), similar relicts were found during research on Otakarova Street in the 1980 s (cf. Frolíková-Kaliszová, 1990; 2020). Our discovery supports the hypothesis that the centre of present-day Uherské Hradisté was previously composed of a network of islands defined by the Morava River channels, which gradually disappeared because of human activity during the Early and especially the High Mediaeval and Modern periods (Frolíková-Kaliszová, 2020).

A stable prehistoric settlement has not yet been proven on St. George's Island, only a few isolated artefacts in secondary positions have been recorded (cf. Procházka and Havlíček, 1996; Frolíková-Kaliszová, 2020). Our observations have pushed the boundary of unspecified human activities to the 6th–7th centuries CE ('Prague-type' culture period). Indeed, a layer of charcoal (Fig. 6A) and the pollen record indicate a weakly human affected forested floodplain in this period. The nearby Early Slavic settlement was documented in Zlechov (Zeman et al., 2006), Staré Město (Hrubý, 1965), Ostrožská Nová Ves (Galuška, 1990) as well as in Uherské Hradisté-Sady (Fig. 2A) (Marešová, 1985).

The dating of the following human activities linked to the formation of the oldest DE (SU 8, P1) is not entirely clear, as the calibrated age (95.4 % probability) presents a timeframe reaching from the second half of the 7th to the second half of the 9th century CE. The modelled age (68.3 % probability) is noticeably shorter and falls from the last third of the 7th century to the first third of the 8th century CE (SM 2), which could be associated with the Early Hillfort period. Human impact on the landscape gradually increased during this period including deforestation in the surrounding. A few fragments of metallurgical waste already indicate the presence of craft workshops in the vicinity of studied area. However, direct evidence of metallurgical facilities on St. George's

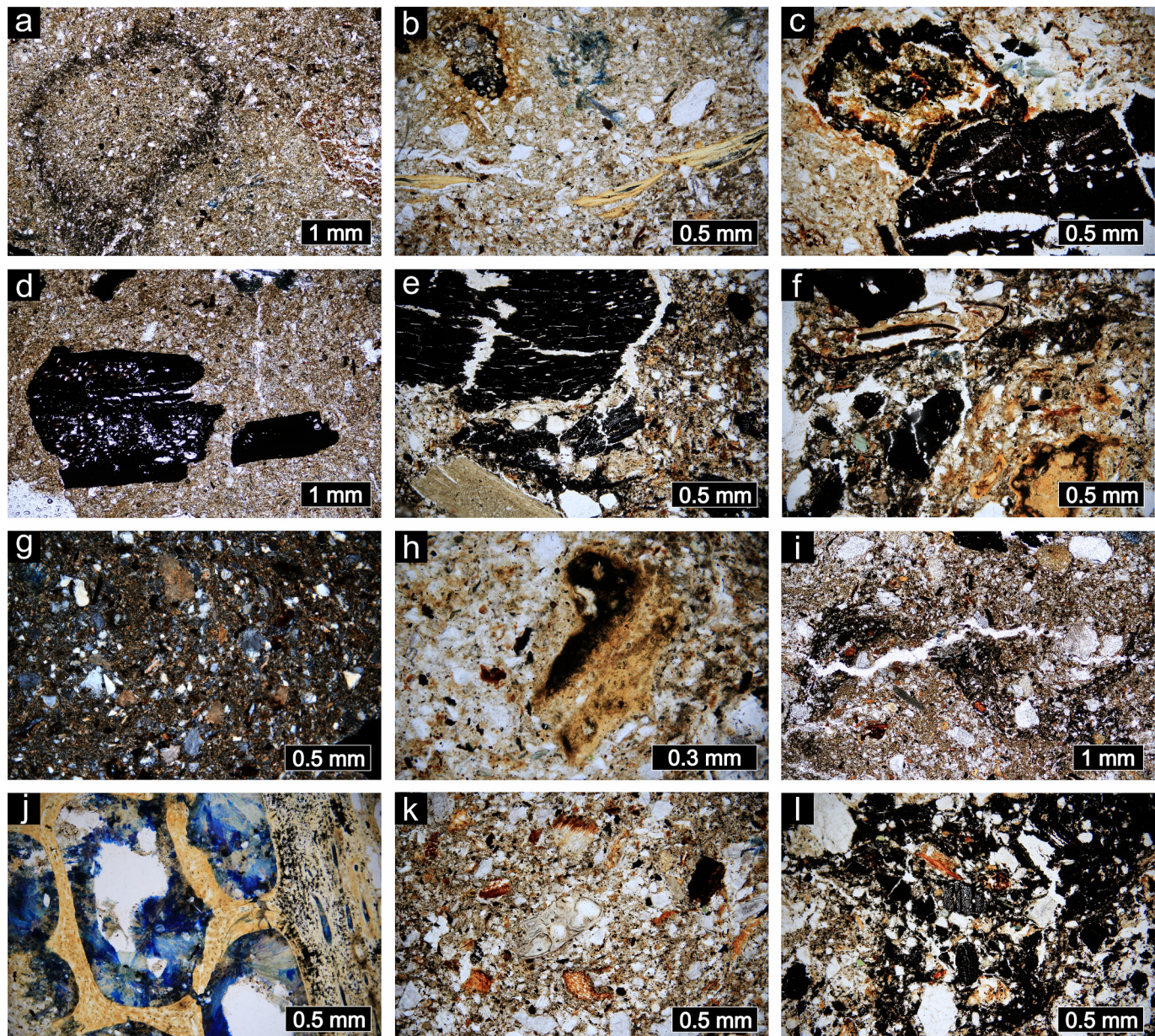


Fig. 10. a – Channel walls coated with fine organic-rich soil material, exhibiting intensive bioturbation in Dark Earth (DE), stratigraphic unit (SU) 8, profile (P) 1, observed in transmitted polarized light (PPL). b – Poorly sorted silt with occasional intrusions of sand, DE, SU 8, P1, in PPL. Note the snapped or crushed unburned bone fragment, metallurgical waste, vivianite, and humus-enriched material. c – Fragment of slag and charcoal, DE, SU 8, P1, in PPL. d – Typical fragmentation of charcoal that entered the soil through poaching, DE, SU 8, P1, in PPL. e – Charcoal and charred black material with a ceramic fragment, DE, SU 8, P2, in PPL. f – Charred black material, charcoal, partially decomposed organic matter, and a fragment of coprolite, DE, SU 8, P2, in PPL. g – Calcareous ashes mixed in moderately sorted silt, DE, SU 6, P1, observed under crossed polarized light (XPL). h – Fragment of omnivore/carnivore coprolite, DE, SU 6, P1, in PPL. i – Convulsions of soil material caused by disturbance of the walking surface, DE, SU 5, P1, in PPL. j – Bone encrusted with vivianite crystals, DE, SU 5, P1, in PPL. k – Glass-like silica indicating high-temperature heating, typically associated with metallurgical activities, DE, SU 5, P1, in PPL. Note the microcharcoal fragments, partially decomposed organic matter, and articulated phytoliths in the upper part of the thin section. l – Charred black material containing charcoal, DE, SU 5, P1, in PPL.

Island is still lacking for this period. Nevertheless, insights into the nature of the earliest iron smelting furnaces can be drawn from other Moravian sites (cf. Merta, 2012). Considering the absence of any archaeological findings, a closer interpretation of human activities is problematic.

The human impact on the landscape intensified from the second half of the 8th century CE (Early Hillfort period), reflected in the formation of several DE layers associated with settlement activities. The situation varied spatially because of the site's geomorphology. While two DEs (SU 6 and 5) in Room 4b, P1 (Fig. 3B and 6A) resulting from multiple phases of anthropogenic activities combined with significant bioturbation

formed in a temporary flooded channel, one (SU 7) of the three DEs (SU 8–6) in Room 3 (P2) situated close to the bank (Fig. 3C and 6A), is attributed to a single dump, possibly related to the elevation of the terrain for flood protection (e.g. Nicosia et al., 2012). This part of the stratigraphy differs significantly in the central area of the site, P3 (Room 4a/4b, Fig. 6A), where it was identified as one DE containing numerous archaeological artifacts, covering the oldest archaeological features sunk into the subsoil. Archaeobotanical and micromorphological results indicate the studied area was an open space with local ruderal vegetation, intensively trampled/poached. The presence of posts and stake holes from above-ground structures (Fig. 4) could originate from a

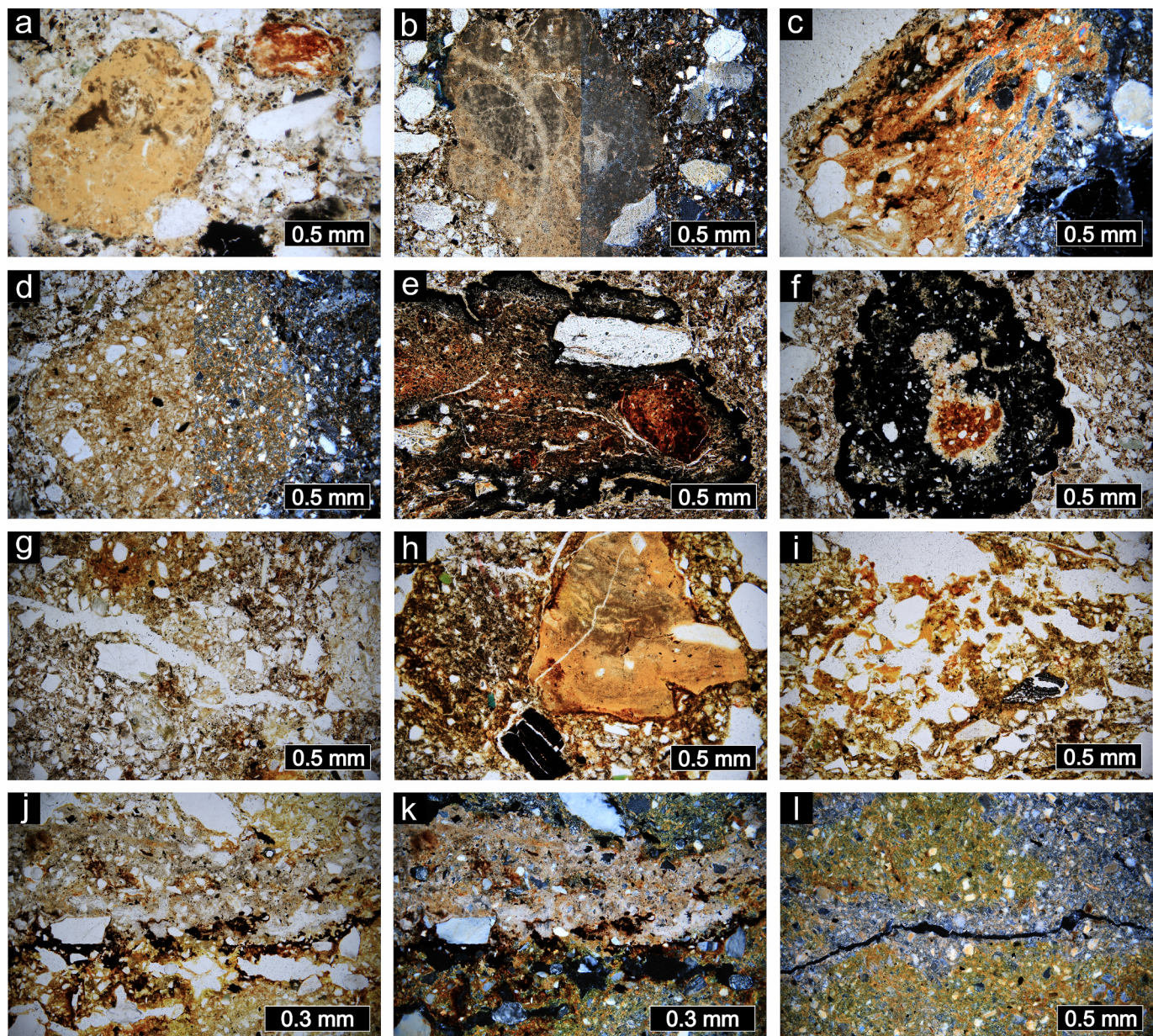


Fig. 11. a – Coprolite fragment, charcoal, and decomposed organic matter, stratigraphic unit (SU) 5, profile (P) 2, observed in transmitted polarized light (PPL). b – Mortar fragment, Dark Earth (DE), SU 3, P1 in PPL (left) and in crossed polarized light (XPL) (right). c – Daub, DE, SU 3, P1, in PPL (left) and XPL (right). d – Earthen-based construction material, DE, SU 3, P1, in PPL (left) and XPL (right). e – Slag fragment, DE, SU 2, P1 in PPL. Note black FeO glassy matrix with dendritic structure and silica sand used for cleaning iron. Orange colour is caused by oxidation. f – Fragment of metallurgical waste, DE, SU 2, P1 in PPL. g – Phosphatic nodule, plane void evidencing trampling, DE, SU 3, P2, in PPL. h – Coprolite and charcoal fragments, DE, SU 2, P3, in PPL. i – Phosphatic coatings, charcoal, DE, SU 2, P3, in PPL. j – High Mediaeval floor layer rich in Ca containing calcareous ashes and charcoal, representing either accumulation of residues from domestic human activities or the remnants of maintenance events, SU 1, P3, in PPL. k – The same photo in XPL. l – Plane void in floor surface evidencing trampling, SU 1, P3, in XPL.

construction for strengthening the channel bank by stakes. A similar arrangement near the channel was identified ca. 150 m from studied site, (Snášil and Procházka, 1981; Procházka and Snášil, 1983; Snášil and Procházka, 1984; Snášil, 1987; Frolíková-Kaliszová, 1990; 2020).

In the DE dated to the end of 8th century CE (SU 5, P1), small pieces of daub and the absence of mortar suggest existence of buildings constructed using wood/wattle and clay at this occupation stage (e.g. Galuška, 2017). This is a phenomenon that is recurrently observed in mediaeval Dark Earth all over Europe (see for instance: Nicosia et al., 2017; Macphail and Devos, 2023). Some artefacts, including an iron spur fragment (Fig. 13A: 1), an iron horse bit (Fig. 13A: 10), a bronze bracelet fragment (Fig. 13A: 9), a complete brass bracelet (Fig. 13A: 2) and a silver belt buckle pin (Fig. 13A: 8) or even a counterfeit gold-

plated Arabic coin (Fig. 13A: 19) dated to 166 AH, which corresponds to August 782 to August 783 CE (determined by M. Daňhel in 2024), indicate the presence of socially higher-ranking individuals on the island in this period. Previous research in the southwest corner of Mariánské Square revealed workshops for processing bones, horns, and antlers, as well as a blacksmithing and non-ferrous metal production (Snášil et al., 1984; Frolíková-Kaliszová, 2020). Slag fragments recognised by micro-morphology (Table 2) could therefore correspond to metallurgical activity and the presence of craft workshops in the proximity. The production could be linked to market exchange which generally facilitates the advancement of specialised production in agricultural and craft sectors by directly mobilising resources from producers and enabling households to acquire necessary goods (Minc, 2006). This market

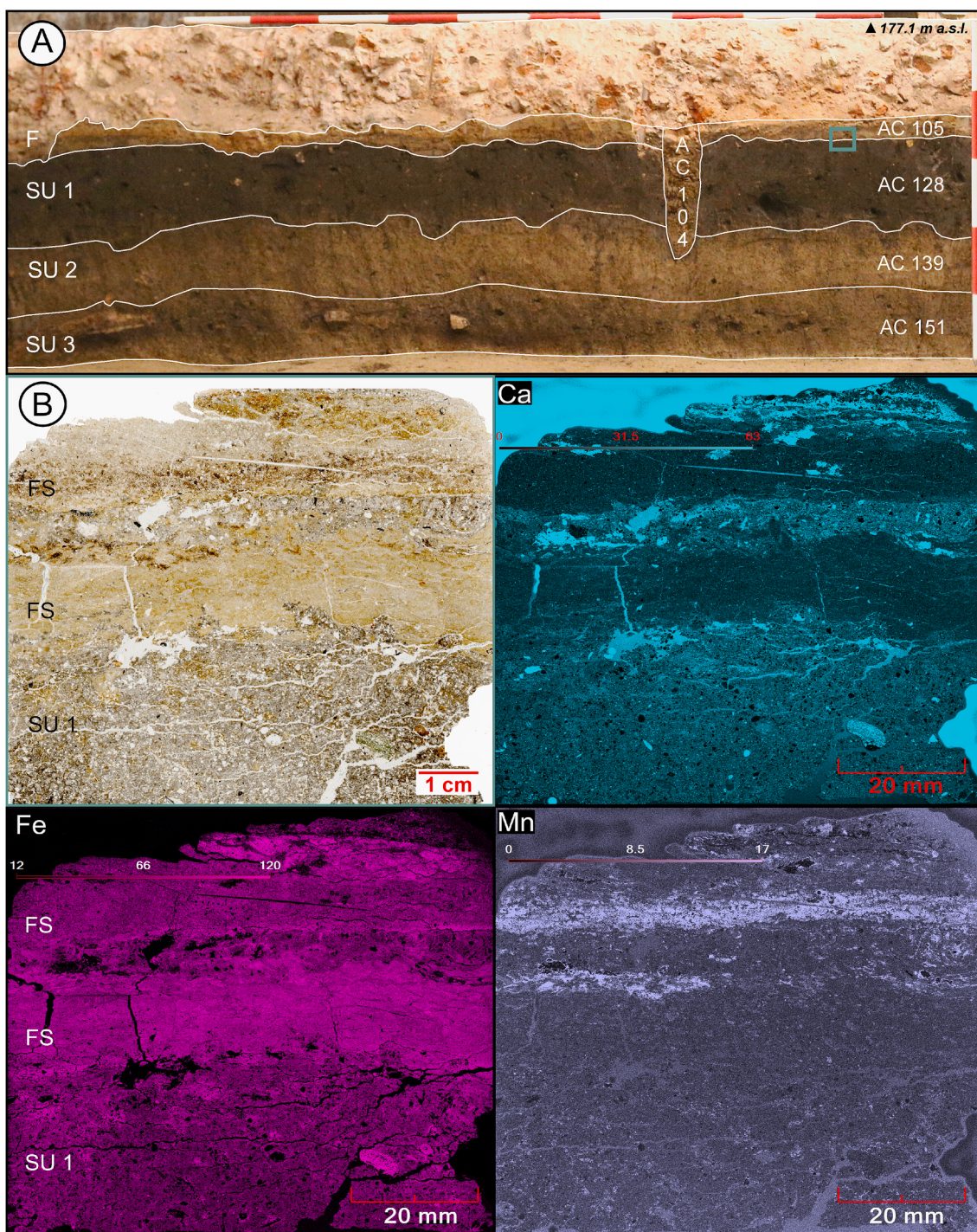


Fig. 12. A. – Photo of the studied Profile 3 in Room 4 (a/b) with marked position of thin section sample from High Mediaeval floor and Dark Earth (SU 1). B – Scan of thin section, with selected µXRF images distinguishing floor surface (FS) and occupation and/ or maintenance phases.

exchange or even marketplace could exist as early as the 8th century on St. George's Island. A market based on long-distance trade facilitated the emergence of a local social elite, raising the question of whether the development of the Staré Město–Uherské Hradiště agglomeration might have followed a different trajectory than previously assumed (cf. Galuška, 2013).

New DEs formed probably from the first half of the 9th century CE (Middle Hillfort period or Great Moravia). Notably, flood sediments (SU 4, P1 and 2; SU 3, P3) separating two main phases of an Early Mediaeval settlement, were documented in nearly all previous excavations in the city centre (Kuchař, 2023; Frolíková-Kaliszová, 2020), indicating that

the flood event(s) affected the entire St. George's Island area. The situation again varies within the investigated area (Fig. 6A). Although three different DEs (SU 3–1) developed in the channel (P1), just one DE horizon (SU 2) was documented in the central part (P3). The channel was gradually filled in, either spontaneously or at some episodes intentionally, as documented by the lowest DEs, and lost its function. It contains a lot of indicators for cultivation, suggesting extensive farming in the surrounding area but as shown by the micromorphological data, not directly in the studied area. Further development indicates an open space still intensively influenced by various human activities. The DEs (SU 3–1, P1) contained a wider range of typologically diverse

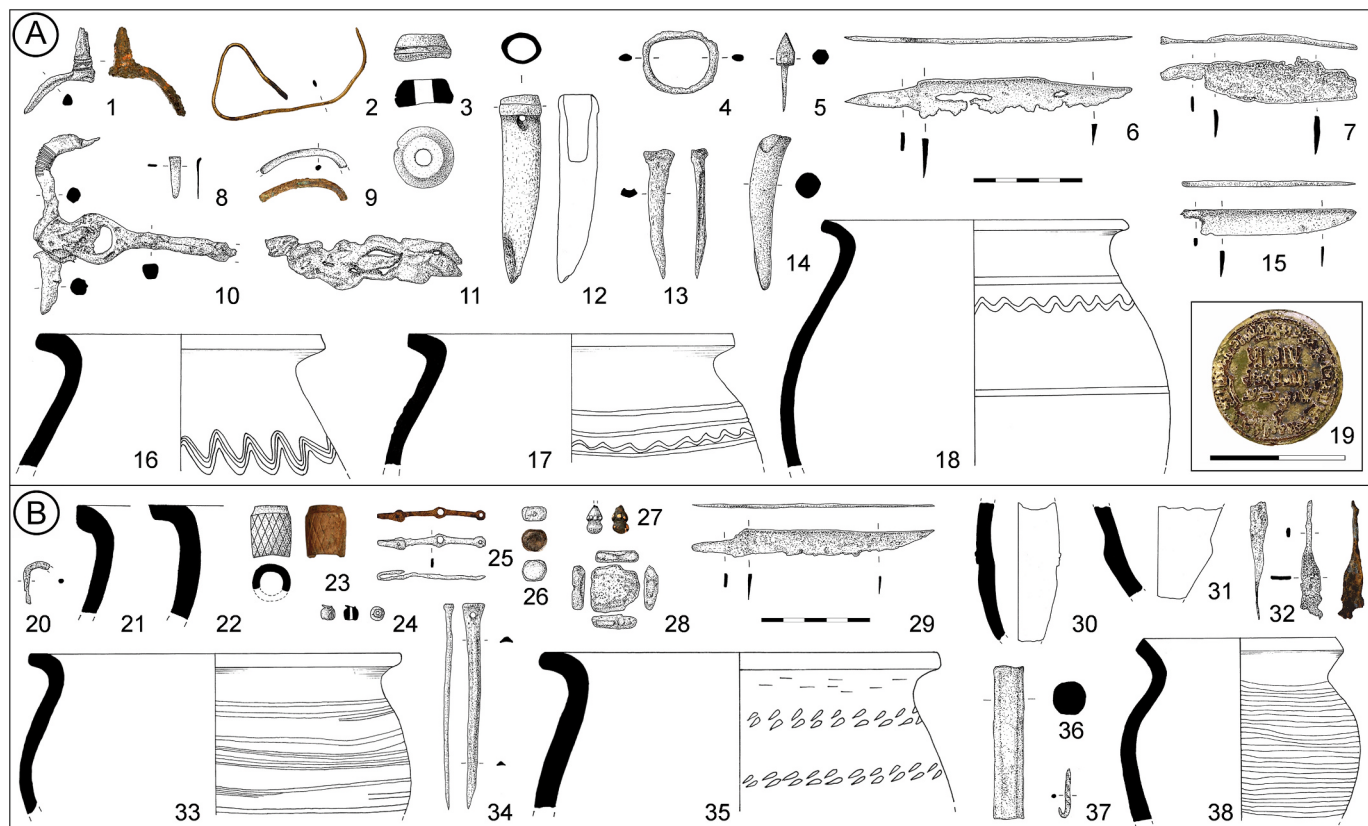


Fig. 13. Selected archaeological finds. A – Older phase of Early Mediaeval settlement from the second half of the 8th century to the beginning of the 9th century CE (archaeological context 151). B – Younger phase of Early Mediaeval settlement from the second half of the 9th century (archaeological context 128). Materials legend: 1, 2, 4–11, 15, 19, 20, 25–29, 32, 36, 37 – metal artefacts; 16–18, 21, 22, 33, 35, 38 – ceramic vessels; 30, 31 – crucibles; bone and antler artefacts – 12–14, 23, 34; 3 – clay whorle; 24 – glass bead.

archaeological finds than the previous cultural layer, although the finds were less numerous. Noteworthy are fragments of lime mortar and plaster (Fig. 11b), indicating the destruction of unspecified structure(s) nearby and thus a spatial re-organisation of the area. A preliminary analysis of construction element imprints suggests that some mortar pieces bonded stones, while other pieces with wattle impressions came from a wooden structure. Similar constructions were identified at Early Mediaeval agglomerations of Pohansko near Břeclav, Staré Město and Mikulčice (e.g. Galuška and Poláček, 2006; Macháček et al., 2014). Thus, the site provides evidence of the advanced building techniques used during the Great Moravian period, incorporating wattle with mortar in their architectural practises (whether sacral or secular), highlighting the island's significant role within the Staré Město–Uherské Hradiště agglomeration.

In addition to common everyday items, the DE contained metal artefacts (Fig. 13B) and a damaged glass bead (Fig. 13B: 24) and a fragment of an iron currency bar (Fig. 13B: 32), considered a form of pre-coinage currency in Moravia (e.g. Hlavica et al., 2020; Hlavica and Bárta, 2021). A unique find is a flat, stick-like object with three copper holes, that is preliminarily interpreted as a balance arm (Fig. 13B: 25). There were several small, cut pieces of lead (Fig. 13B: 26, 28) nearby, which might have served as weights. Great Moravia had a sophisticated economy, which included long-distance trade connections with Western and Eastern Europe and the establishment of marketplaces. It is assumed that in the 9th century CE, there was one such market in the centre of the nearby Staré Město (Kouřil, 2014; Hlavica et al., 2023). All above-mentioned uncovered artefacts, micromorphological observation evidencing artisanal waste (cf. Wouters et al., 2017), the position in the corner of recent-day square (Fig. 2B) and the evidence of the existence of markets in the Great Moravia period can support the hypothesis

regarding the presence of a marketplace or trade/exchange place in the vicinity of the studied area. The Mariánské Square hosted a town market from the High Middle Ages to the early 20th century CE (Čoupková and Čoupek, 2007), which could reinforce the hypothesis regarding a previous marketplace in this area.

The uppermost DE (SU 1, P1; SU 2, P3; Fig. 6A), rich in nutrients, was formed after the Great Moravian settlement probably from the 10th century CE (Fig. 8). Because of the lack of dates, we cannot further detail the formation period. Human impacts on the landscape decreased, and the site was likely abandoned or used only sporadically. This finding is consistent with the results of previous research in the centre of Uherské Hradiště, where we currently lack intensive evidence of settlement from the Late Hillfort Period (10th–12th centuries; Procházka and Doležel, 2001; Frolíková-Kaliszová, 2020). If any human activities took place on St. George's Island, they were probably related to the surrounding settlements in nearby Staré Město, where the population moved from its original central location to the areas known as 'Na Dědině' and 'Na Zahrádkách', and/or in Uherské Hradiště-Sady 'Špitálky' (Galuška, 200b; Fig. 2A). A similar scenario is known from the Early Mediaeval agglomeration of Pohansko, which was abandoned in the 10th century CE, leading to the settlement expanding into the surrounding areas (Dresler, 2016).

On the parcel that we examined, oak piles used to anchor an unspecified structure dated back to the first third of the 13th century CE (Late Hillfort period) were driven into older Early Mediaeval DE in room 6. The structure could be hypothetically linked to the existence of a small fishing village with a chapel referenced by written sources even before the establishment of the royal town itself in CE 1257 (Mitáček and Procházka, 2007) and could be assessed as the initial phase of urbanisation in Uherské Hradiště. The remains of High Mediaeval

buildings/houses have survived here only in fragments as oak piles dated to CE 1210–1281, thin floor horizons (for details see Section 4.2.3) and a few shallow features sunk into the uppermost DE. We also documented fence made of thin stakes woven with willow twigs and organic-rich deposits interpreted as a manure heap (Bartík and Chrátek, 2018). Wattle fences dividing areas into small plots are typical of early towns including Uherské Hradiště (Procházka, 2022; Procházka and Snášil, 1984; Mitáček and Procházka, 2007).

6. Conclusion

The archaeological investigations conducted at Mariánské Square provided significant insights into the landscape, paleoenvironment, and human settlement development on St. George's Island in Uherské Hradiště. The geomorphological and environmental conditions of the island located in the river's floodplain and the building foundations directly built on contributed to the preservation of DEs and archaeological contexts that would have otherwise been lost because of pedogenesis. By applying a diverse range of geoarchaeological, paleoenvironmental and dating methods, we can now interpret the obtained data within broader historical and spatial context. The micromorphological analysis and archaeological investigation provided greater stratigraphic details and enhanced the interpretation of both natural and human activities from proto-urban to urban societies in the 6th–14th centuries AD, which included occupation phases and periods of soil formation interspersed with episodes of flooding and floodplain aggradation. The first stable settlement of St. George's Island began at the transition of the 7th and 8th centuries AD. The area under study represented a trampled open space close to metallurgical workshops. More mature and more human-influenced DEs formed from the second half to the end of 8th century CE. The presence of specific artefacts linked to higher-status individuals and evidence of specialised artisanal activities suggest a complex societal structure in Uherské Hradiště with significant economic and social interactions based on the development of controlled long-distance trade. At the end of the 8th and 9th centuries CE the site was flooded. However, settlement in the area was renewed. New DEs developed from the first third of the 9th century CE when the site belonged to an important settlement area of the Great Moravian Empire. The study of these DEs revealed a series of activities such as levelling of the terrain (mainly from building rubble containing mortar) and the associated re-organization of the space, cultivation in the vicinity as well as the proximity of craft workshops and the presence of a marketplace. The site was already probably an essential trading centre in this period. From the beginning of the 10th century CE, the site was probably abandoned. The settlement re-established at the beginning of the 13th century CE representing the first traces of urbanisation and the early formation of mediaeval city Uherské Hradiště founded after CE 1257. The town was hit by another flood at the turn of the 13th and 14th centuries AD, probably caused by intensification of settlement activities in the catchment.

To gain a comprehensive understanding of the Early Mediaeval functioning of the island, uncovering a larger portion of the production and exchange areas, particularly metallurgical sites, is crucial. Future research should also focus on interpreting structures containing significant amounts of mortar or lime plaster, as these could indicate the presence of churches, palaces, or other important buildings in the period of Great Moravia. Discovering and interpreting these structures would significantly enhance our understanding of the island's role and the broader settlement dynamics during this period.

CRediT authorship contribution statement

Katarína Adameková: Writing – original draft, Visualization, Methodology, Investigation, Formal analysis, Conceptualization. **Jaroslav Bartík:** Writing – original draft, Visualization, Investigation, Conceptualization. **Jan Petřík:** Writing – review & editing,

Visualization, Methodology, Investigation. **Yannick Devos:** Writing – review & editing, Supervision. **Líbor Petr:** Writing – original draft, Investigation, Formal analysis. **Petr Kočář:** Writing – original draft, Formal analysis. **Romana Kočárová:** Formal analysis. **Tomáš Chrátek:** Investigation. **Marcin Frączek:** Formal analysis. **Michał Kurka:** Formal analysis. **Miloslav Pouzar:** Formal analysis.

Declaration of competing interest

The authors declare that they have no known competing financial interests or personal relationships that could have appeared to influence the work reported in this paper.

Acknowledgements

K. Adameková would like to thank Christine Pümpin, David Brönnimann, Hans Huisman and Kristin Ismail-Meyer for consulting micromorphological samples. Many thanks to Barbora Wouters, who gave her the opportunity to advance my knowledge in the field of micromorphology, Luc Vrydaghs, who introduced her to the issue of phytoliths and Rosa Maria Poch Claret for consulting soil formation processes. The authors further thank Rudolf Procházka and Miroslav Daňhel for expert advice and consultations and to Martina Kudlíková and Markéta Kamenská for mediation of proofreading. This publication was supported by the institutional support RVO: 68081758 – Czech Academy of Sciences, Institute of Archaeology, Brno and by projects OP JAK under Grant No. CZ.02.01.01/00/22_008/0004593 “Ready for the future: understanding long-term resilience of the human culture (RES-HUM) and LM2023037 from the Ministry of Education, Youth and Sports of the Czech Republic.

Appendix A. Supplementary data

Supplementary data to this article can be found online at <https://doi.org/10.1016/j.catena.2025.108734>.

Data availability

Data will be made available on request.

References

- Adameková, K., Bartík, J., Petřík, J., Kočář, P., Kočárová, R.. Supplemental Material for Anthropogenic soils and sediments from historical trade hub on the bank of Morava River in Uherské Hradiště (Czech Republic): Archives of mediaeval landscape, environment and settlement dynamics [Data set]. Zenodo. <https://doi.org/10.5281/zenodo.1471177>.
- Adameková, K., Petřík, J., 2022. The myth of ‘Bohunician soil’: A re-evaluation of the MIS 3 palaeosol record at the Brno-Bohunice site (Czechia). Catena 2017, 106510. <https://doi.org/10.1016/j.catena.2022.106510>.
- Asare, M.O., Horák, J., Šmejda, L., Janovský, M., Hejman, M., 2020. A medieval hillfort as an island of extraordinary fertile Archaeological Dark Earth soil in the Czech Republic. Eur. J. Soil Sci. 72, 98–113. <https://doi.org/10.1111/ejss.12965>.
- Bartík, J., Chrátek, T., 2018. Uherské Hradiště (Uherské Hradiště District). Přehled výzkumu 59 (2), 276–277.
- Beug, H.-J., 2004. Leiträfden der Pollenbestimmung für Mitteleuropa und angrenzende Gebiete. Verlag Dr. Friedrich Pfeil, München.
- Bloemendal, J., Liu, X., Sun, Y., Li, N., 2008. An assessment of magnetic and geochemical indicators of weathering and pedogenesis at two contrasting sites on the Chinese Loess plateau. Palaeogeogr. Palaeoclimatol. Palaeoecol. 257 (1–2), 152–168. <https://doi.org/10.1016/j.palaeo.2007.09.017>.
- Borderie, S., 2011. L'espace urbain entre antiquité et Moyen âge. Analyse géoarchéologique des terres noires. Université de Paris 1, Paris. Etudes de cas. Unpublished PhD thesis.
- Borderie, Q., Devos, Y., Nicosia, C., Cammas, C., Macphail, R.I., 2015. Les terres noires dans l'approche géoarchéologique des contexts urbains. In: Carcaud, N., Arnaud-Fassetta, G. (Eds.), La géoarchéologie française au XXIe siècle, CNRS éditions, pp. 247–258.
- Bortolini, M., Agnolotto, F.C., Argiridiadis, E., Nicosia, C., McWethy, D.B., Devos, Y., Stortini, A.M., Baldan, M., Roman, M., Vendrame, T., Scaggiante, R., Bruno, B., Pojana, G., Battistel, D., 2022. Insight into the carbonaceous fraction of three cultural layers of different age from the area of Verona (NE Italy). Catena 217, 106453. <https://doi.org/10.1016/j.catena.2022.106453>.

- Svobodová, H., 1990. Vegetace jižní Moravy v druhé polovině prvého tisíciletí. *Archeologické rozhledy XLII*, 170–230.
- Svitavská-Svobodová, H., 2011. Pylová analýza vzorků z archeologického výzkumu Uherské Hradiště. Unpublished report, Otakarova ul.
- Tolasz, R., 2007. *Atlas podnebí Česka. Český hydrometeorologický ústav and Univerzita Palackého v Olomouci, Praha and Olomouc*.
- Tys, D., Wouters, B., 2016. Antwerp (Belgium) – A ninth century Viking town? From early medieval trading place to Ottonian power centre. In: Kalmring, S., Hedenstierna-Jonson, C., Holmquist, L. (Eds.), *New Aspects on Viking-age Urbanism c. AD 750-1100: Proceedings of the International Symposium at the Swedish History Museum, April 17–20th 2013*. Stockholm: Archaeological Research Laboratory, University of Stockholm, pp. 195–202.
- Nalepka, D., Walanusz, A., 2003. POLPAL – Program for counting pollen grains, diagram plotting and numerical analysis, *Acta Palaeobot. Suppl. 2*, 659–661.
- Wentworth, C.K. 1922. A scale of grade and class terms for clastic sediments. *The Journal of Geology* 30 (5), 377–392. <https://doi.org/10.1086/622910>.
- Wouters, B., Devos, Y., Milek, K., Vrydaghs, L., Bartholomieux, B., Tys, D., Moolhuizen, C., van Asch, N., 2017. Medieval markets: A soil micromorphological and archaeobotanical study of the urban stratigraphy of Lier (Belgium). *Quat. Int.* 460, 48–64. <https://doi.org/10.1016/j.quaint.2017.03.002>.
- Wouters, B., Devos, Y., Vrydaghs, L., Ball, T.B., De Winter, N., Reygel, P., 2019. An integrated micromorphological and phytolith study of urban soils and sediments from the Gallo-Roman town Atuatuca Tungrorum, Belgium. *Geoarchaeology* 34, 448–466. <https://doi.org/10.1002/gea.21722>.
- Zeman, T., 2006. Sídlistě z pozdní doby římské ve Zlechově. Stav zpracování, východiska a cíle projektu. In: Droberjar, E., Lutovský, M. (Eds.), *Archeologie barbarů 2005*, Kounice, 451–469.